PLASMA SPOUTED BED CALCINATION

OF LAC DORÉ VANADIUM ORE CONCENTRATE

A

THESIS

by

JAN KREIBAUM, B. Eng.

Department of Chemical Engineering - McGill University

Under the supervision of Dr. R.J. Munz

Submitted to the Faculty of Graduate Studies and Research of McGill University in partial fulfillment of the requirements for the degree of Master of Engineering.

McGill University
Montreal, Canada

December 1986

To my

wife and parents

ABSTRACT

A plasma spouted bed reactor was designed and built to calcine concentrated vanadium ore to extract vanadium in the form of sodium metavanadate. A 10 kW-dc plasma torch was used with nitrogen or argon as the plasma gas. Air was injected into the spout region to provide oxygen for the roasting reactions. Experiments were performed to assess the stability of the reactor in batch operation as a function of operating conditions and concentrate particle size. Very fine concentrate (50 % below 40 microns) gave unstable operation even at low mean bed temperatures due to localized melting. Larger particles (50 % below 60 microns) and micro-agglomerated particles gave a wider range of stable operating conditions. Conversions of the vanadium oxide to sodium metavanadate by reaction with sodium bicarbonate were as high as 40 % with final bed temperatures up to 950 K after 40 minutes of reaction. The use of a spout-fluidized bed is proposed to improve circulation rates which will allow higher mean temperature operation.

Resumé

Un réactor à jet utilisant une torche à plasma a éé conçu et construit pour la calcination du minerai de vanadium pour extraire le vanadium sous forme de métavanadate de sodium. Le gaz plasmagène de la torche 10 kW-dc est constitué soit d'azote, soit d'argon. On inject de l'air dans la région du jet pour fournir l'oxygène nécessaire aux réactions de grillage. Les expériences ont pour but d'estimer la stabilité du réacteur en opération discontinue, en fonction des conditions opératoires et de la taille des particules. Les plus petites particules (50 % inférieures à 40 micromètres) conduisent à une instabilité du processus, meme aux basses températures moyennes dans le lit. Ce phénomène s'expliquerait par des fusions localisées. Les plus larges particules (50 % inférieures à 60 micromètres) et les micro-agglomérats de particules conduisent à un plus large domaine de conditions opératoires stables. Le rendement de conversion de l'oxide de vanadium en métavanadate par réaction avec le bicarbonate de sodium atteint 40 % avec des températures finales dans le lit supérieures à 950 K après 40 minutes de réaction. L'utilisation de lit fluidisé à jet est proposée pour améliorer les vitesses de circulation, ce qui permettra s'admettre des températures moyennes opératoires plus élevées.

Acknowledgements

A single author appears on the front page of this thesis. However, to say that it has been completed by this author alone would be false. So many people have directly and indirectly contributed to this work that it becomes hard to remember them all (especially for absent-minded me). The following is an attempt to name as many of these people as possible. Warm thanks to all of you.

To start, where I would I be without my adviser, Dr. Munz. A special thank you for all your help.

Dr. Malinsky from the Centre de Recherches Minérales.

The best plasma lab in the world (my second home); Gang-Qian, Earle, Oliver, Peter P., Paul, Roberto. I'll miss you.

All the others; Imtiaz, Omar, Ian, John Mac, John F., Bing, Cermal, Peter T., Ira, Stuart, Maysaa, Larry, Bruno, Gino.....
....the list goes on and on.....

All the people in the Chem. Eng. Dept. who were always there when

I needed them; Jean, Dr. Gauvin, Dr. Berk, Pat, Anne, Louise and everybody else.

The guys in the machine shop, who never failed to fascinate me with their ingenuity and craftiness; Mr. Krish, Alain, Don, Walter, and Herb.

From the Université de Sherbrooke, Dr. Boulos for his excellent torch, and Dr. Jurewicz for all his valuable advice.

Monique Riendeau and Michel Leroux in the Dept. of Mining & Metallurgy, who sacrificed so much time for me.

My father and mother, without whom I wouldn't even be here. Domo. Bell Canada loves us.

To my wife, Jik-ja. My gratitude does not fit into this thesis. The future is ours.

TABLE OF CONTENTS

LIST OF FIGURES

LIST OF TABLES

CHAPTER I

GENERAL INTRODUCTION

Introduction

The Lac Doré region of Québec boasts one of the largest vanadium ore deposits in the world. The Centre des Recherches Minérales, Québec, has looked into the best ways of making use of these deposits.

A common route to vanadium recovery is the calcination of the ore concentrate with a sodium salt (rendering the vanadium pentoxide water-soluble) followed by a leach. To contact the ore with the sodium salt at the necessary high temperatures, two conventional processes can be considered. They involve either the use of a rotary kiln or a fluidized bed calciner. The former is the more established technology. The latter seems to be more promising as it is smaller, more cost-efficient and allows for higher throughputs. The use of a plasma torch as the source of heat entails several advantages: it can easily generate the necessary temperatures, it is compact, it uses electricity (cheap and in surplus in Québec) and it is a likely candidate for process automation.

It is desired to develop a process for shorter residence times to reduce equipment capital costs and increase throughputs. Plasma can be used as a heat source and reactant but cannot be

easily used to feed a fluidized bed. A spouted bed can be more effectively matched with a plasma torch. The purpose of this project is to investigate the feasability of using a plasma spouted bed reactor to accomplish the calcination reaction.

CHAPTER II

LITERATURE REVIEW

1. Vanadium

1.1 Properties of Vanadium

Vanadium has an atomic weight of 50.9414, a melting point of 1890 $\pm$ 10°C, a boiling point of 3380°C, and a specific gravity of 6.11 (at 18.7°C). It was first discovered in 1801 by del Rio, who however, mistakenly identified it as impure chromium. It was rediscovered in 1830 by Selfstrom who named it after the Scandinavian goddess Vanadis because of its beautiful multi-colored compounds. It was first isolated in a pure form in 1867, by reducing the chloride with hydrogen.(39)

Vanadium is found in 65 different minerals. It is also found in phosphate rock, certain iron ores, and is present in some crude oils in the form of organic complexes. Natural vanadium is a mixture of two isotopes, V^{50} (0.24%) and V^{51} (99.76%). Pure vanadium is a bright white metal, and is soft and ductile. It has good corrosion resistance to alkalis, sulfuric and hydrochloric acid, and salt waters, but it oxidizes readily above 660°C. The metal has good structural strength, and a low-fission neutron cross-section, making it useful in nuclear applications. (39)

1.2 Uses of Vanadium

Vanadium is used in producing rust-resistant, spring, and high-speed tool steels. It is an important carbide stabilizer in making steels. About 80% of the vanadium now produced is used as ferrovanadium or as a steel additive. Vanadium foil is used as a bonding agent in cladding titanium with steel. Vanadium pentoxide is used in ceramics and as a catalyst. It is also used as a mordant in dyeing and printing fabrics. Vanadium and its compounds are toxic and should be handled with care.(39)

1.3 Vanadium Resources

1.3.1 World Deposits

Magnetite deposits form the most important source of vanadium. Approximately 75% of all vanadium is expected to come from this source. Notable vanadium deposits around the world are: clay sands of Arkansas (1% V_2O_5, production of 4500 tons V_2O_5/year), the mineral deposits of Colorado (-0.5% V_2O_5, production of 3200 tons V_2O_5/year), the vanadiferous shale deposits of Nevada (-1% V_2O_5), the mineral deposits of South Africa (0.5% V_2O_5), the mineral deposits of Chile (0.3%-0.4% V_2O_5), and the oil deposits of Venezuela (100-500 ppm, 3000 tons

V_2O_5/year in 1983). A more detailed table configuring deposits in the United States is presented in Table I.(24,25)

In the United States, the Arkansas clay deposits are the only deposits used solely for the production of vanadium. This mineral has some disadvantages when compared to titaniferous magnetites. Primarily, its high content of SiO_2 makes the extraction of vanadium difficult and costly. The vanadiferous shale deposits of Carlin, Nevada contain approximately 1% V_2O_5. The principal minerals are illite, dolomite and quartz. The vanadium is largely substituted for aluminum in the illite. The Carlin deposit poses two major problems in the extraction of the vanadium which are absent at Arkansas. Firstly, the deposit contains a highly carbonaceous fraction. The carbon is an oxygen consumer, and any CO formed can act as a vanadium reductant. Secondly, the high calcium content of the ore leads to the formation of water-insoluble vanadates. This deposit has not been developed beyond the explorative stage. Other deposits in the United States are not exploited due to either low concentrations of vanadium, or small overall deposits.(9,24)

The largest source of vanadium in the world is found in titaniferous magnetite deposits (such as in Lac Doré). Vanadium exists in the magnetite structure substituted for ferric iron,

TABLE I

Vanadium Ore Deposits in the U.S.

Location	Vanadium Content % V_2O_5	Known Reserves million lbs.	
Arkansas[1]	0.71 - 1.25	60	(0.14%)
Colorado, New Mexico[1]	0.11 - 0.89	90	(0.21%)
Idaho and Wyoming[2]	0.7 - 0.89	600	(1.40%)
Idaho[3]	0.14 - 0.82	254	(0.59%)
Nevada[4]	0.71 - 1.07	20	(0.05%)
California[4]	0.54	60	(0.14%)
New York[4]	0.27 - 0.54	500	(1.17%)
Wyoming[4]	0.04 - 0.64	500	(1.17%)
Rhode Island[4]	0.30	42	(0.10%)
Minnesota[4]	0.09 - 0.2	180	(0.42%)
Alaska[4]	0.04 - 0.36	40,450	(94.65%)
TOTAL U.S.		43,000	(100 %)

[1]vanadiferous clay
[2]vanadiferous shale
[3]vanadiferous phosphate rock
[4]titaniferous magnetite

i.e. $FeO.V_2O_3$ replaces $FeO.Fe_2O_3$. Titanium is generally present as ilmenite ($FeTiO_3$).(24)

1.3.2 Lac Doré Deposits

The Lac Doré region of north-western Québec boasts one of the world's most substantial vanadium deposits. These deposits, 15 miles from the town of Chibougamou were discovered in the sixties. The Ministère de l'Energie et des Ressources du Québec (previously le Ministère des Richesses naturelles) became the owner of the deposits. The Centre de Recherches minérales was asked to study the possibility of processing this ore for economical gains. In 1974 the Société québécoise de l'Exploration minière (SOQUEM) acquired the right of mining and developing the deposit.(24)

The region is estimated to contain up to 73 million tons of mineral ore, which itself contains as much as 270 million kg of vanadium. These deposits are found close to the surface and are thus readily accessible for mining. In addition, the region is in an area with a well-developed infrastructure, facilitating the exploitation of the deposits.(24)

Magnetic concentration of this ore can yield a concentrate containing 1.5 % V_2O_5. Table II shows the composition of the

mineral ore both before and after concentration. The value of V_2O_5 is considered acceptable for further processing using the salt roasting and leaching techniques used in Finland and South Africa. The complete composition of the ore is given in Table III.(12,24)

1.3.3 World Market for Vanadium

The United States and Europe are by far the largest consumers of vanadium. Approximately 6 million kg per year are consumed in the U.S., compared with 15 million kg per year in Europe. Both of these major consumers are potentially major importers of Lac Doré vanadium for several reasons: First of all, more than 50% of the vanadium consumed in the U.S. is locally produced, but is of inferior purity compared to Lac Doré vanadium. It is indicated that for higher quality vanadium, importing is cheaper than more extensive and improved processing of local vanadium. Secondly, up to 70% of the vanadium consumed in Europe is imported from the Soviet Union and South Africa. It is not surprising that this situation is not favorable to most European countries.(24)

TABLE II

Composition of Lac Doré Mineral Ore

	Before Concentration %	After Concentration %
V_2O_5	0.65	1.5
Fe	35	65
TiO_2	10	7-9

TABLE III

Complete Composition of Concentrated Lac Doré Mineral Ore

Chemical	Composition %
Fe_{tot}	64.0
Fe_2O_3	56.2
FeO	32.7
Al_2O_3	0.68
V_2O_5	1.47
TiO_2	7.61
SiO_2	1.13
CaO	0.16
MgO	0.435
Na_2O	0.05
K_2O	< 0.01
MnO	0.2
Cr_2O_3	0.13
C	0.02
S	0.025

1.4 Recovery of Vanadium

1.4.1 Conventional Methods

Various recovery methods have proven to be successful in vanadium extraction. Among the more common are several variations of salt roasting followed by water leaching technique (as in the work of this thesis), acid leaching and smelting.

Salt Roasting

Salt roasting and water leaching has proven a very effective method for recovering vanadium from titaniferous magnetite ores. Often, the ore is first concentrated magnetically which not only increases the feed quality but also removes a large amount of gangue constituents such as quartz and silicates which can decrease water leach recoveries. The complete process entails four steps:

1) The ore is preoxidized. In effect, the magnetite is oxidized to hematite, liberating vanadium from the spinel structure. Commonly, the ore is heated with oxygen at temperatures ranging from 800°C to 1100°C.

2) The ore is then reacted with a sodium salt. The vanadium forms a sodium vanadate which is water-soluble.

3) The reacted ore is leached with water. The sodium vanadate is leached into the liquor.

4) The sodium vanadate is purified and converted to V_2O_5.(27,37)

Several factors are of importance in the salt roasting process. A major one is the salt used. Three salts are usually considered: NaCl, Na_2CO_3, and Na_2SO_4. NaCl has the advantage of being cheap, however, it requires the additionof water. In most studies reported, Na_2CO_3 has given the best vanadium recoveries. Na_2SO_4 can give equally high recoveries as Na_2CO_3, but requires higher reaction temperatures. Several studies reported improvements when using various combinations of Na_2CO_3 with NaCl or Na_2SO_4. NaOH has been shown to give good results, however its use is economically prohibitive.(9,14,15,36,37)

With Na_2CO_3, an optimum concentration of salt is approximately 10 % by weight. When using a concentrated ore, recoveries of vanadium are approximately 75% after roasting at 900°C for 1 hour.(14)

Feed preparation may have a significant effect on the yield. In most processes, a finer feed gave better yields due to an increase in contacting area. At the same time, problems with excessive dusting, kiln-lining, and fusing were sometimes experienced. Pelletization of the feed is commonly employed. This eliminates most of the problems mentioned above while intimate contact of the reagents is retained throughout the

process. Problems are sometimes encountered with a lack of strength of the pellets. The pellets must be strong enough to avoid destruction in the furnace, but must still have a suitable porosity for optimum leaching.(9,14)

Various studies examined the effect of the roasting temperature on the degree of recovery. Generally, the minimum temperature necessary for a good recovery of vanadium is around 800°C, improving when raised to 850°C. Some studies show definite recovery improvements when raising temperatures to as high as 1100°C, while in most studies the effect of raising temperatures significantly above 850°C above gave no improvements, and in some cases a decrease was observed. (9,14,33)

Most studies report similar results when investigating optimum roasting times. Whereas good recoveries could be obtained after 30 minutes, the optimum is 60 minutes. Roasting times extending beyond this optimum showed no improvements on recoveries.(9,14,36)

Acid Leaching

Acid leaching technology developed through the increased value of uranium over vanadium. Uranium ores also containing vanadium are leached with strong acids (usually sulfuric) resulting in a liquor rich in uranium, iron, silica, phosphorous

contents and vanadium (usually in the form VO_4). After the uranium has been extracted from the solution, vanadium is precipitated as a 'red cake'. When dried and fused, it becomes the standard 'fused oxide' of commerce and the conventional source of vanadium for ferrovanadium.(7)

1.4.2 Operating Recovery Sites

Major deposits of titaniferous magnetite containing 0.47 % V_2O_5 are found at Otanmaki, Finland. The ore is concentrated to approximately 1 % V_2O_5. The concentrate is then mixed with sodium carbonate and is subsequently pelletized. The pellets are then fired in a vertical furnace at 1200°C. The fired pellets are leached in hot water, dissolving vanadium in the form of ammonium metavanadate. The ammonium metavanadate is finally thermally decomposed to yield V_2O_5.(27)

A process similar to the Otanmaki process is employed in Bushveld, South Africa. The Bushveld ore contains 1.2 - 2.0 % V_2O_5. The ore is fired at 800°C with NaCl. The fired ore is then acid leached with hydrochloric acid.(27)

Also using Bushveld ore, the South African Highveld company has developed a vanadium extraction process. The ore goes through a prereduction step in a rotary furnace followed by a

reduction step in an electric furnace. Up to 90 % of available V is recovered in the melt. Subsequently, the melt is oxidized to form a slag containing 25 % V_2O_5. This slag is then salt roasted following standard technology.(27)

1.4.3 Fluidized Bed Roasting

Several studies have been conducted into methods of extracting vanadium from vanadium-containing ores by using fluidized beds.

Much effort by the Centre de Recherches Minérales (CRM) has been put into studies concerning the Lac Doré vanadium deposits. However, most of it has been limited to evaluating the adaptability of existing technologies, and little has been spent on radically different processes.

The use of a fluidized bed had been considered on various occasions. A proposal had been made together with the Université du Québec (Chicoutimi) to develop a fluidized bed that would allow for the contacting of the concentrated ore with oxygen and a vaporized sodium or metallic salt. Whereas a plasma torch had been suggested as the heat source, only a natural gas combustion torch has been actually tested. The project was eventually abandoned due to the complexities involved.

A certain amount of research has been conducted in the choice of sodium salts. As its main conclusions, CRM reported that Na_2CO_3 is more efficient than NaCl. In addition, the use of NaCl entails the production of corrosive and toxic pollutants (Cl_2, HCl).(24)

At present, the only known commercial application of fluidized beds to extract vanadium from a mineral ore, has been realized by Agnew Clough Ltd. of Australia. In this process, mineral ore that has undergone some prior processing is fed to two fluidized beds. The ore, containing 1.2% V_2O_5, is dehydrated at 500°C in the first fluidized bed. The dehydrated ore is then fed into the second fluidized bed. To obtain the necessary operating temperature of 1200°C, the powdered ore is mixed with Na_2CO_3 and oil. The resulting product is then leached in water, where SiO_2 and Al_2O_3 are precipitated. Vanadium, in the form of ammonium metavanadate is recovered from the remaining solution. This ammonium metavanadate is then decomposed in a standard rotary kiln to produce the desired vanadium (in the form of V_2O_5).(24)

Saha, Misra and Bhatnagar (32) roasted a vanadium ore containing 0.97% V_2O_5 and compositions of Fe and Ti oxides comparable to Lac Doré ore with sodium salt to convert V_2O_5 to

$NaVO_3$. The effect of various factors including temperature, feed size, fluidisation air rate, residence time, and ore/salt ratio was studied.

The charge was prepared by dissolving the salt in water, and then mixing this solution with the ore to form a mud-like slag which was then dried at 110°C. Agglomeration takes place during this process, and the dried mass could be hand-crushed to the desired feed size.

Particles of 125-250 micron, with an ore/salt ratio of 25/3 were roasted for 120 minutes at an air fluidisation rate of 180 lph (at a diameter of 2.54 cm). The temperature was varied from 750°C to 900°C. The conversion ranged from 18.64% at 750°C to 60.38% at 900°C. The conversion did not increase appreciably above 850°C (58.71%).

Five different screen sizes were used: 425-600 micron, 300-425 micron, 212-300 micron, 150-212 micron, and 90-150 micron. Other conditions were 850°C, 120 minutes roasting time and 180-200 lph air flow rate. The conversions were as follows:

TABLE IV

Effect of Particle Size on Conversion

Size	Conversion	Size	Conversion
-25+36	32.2 %	-72+100	55.18%
-36+52	44.15%	-100+172	22.28%
-52+72	48.94%		

The 125-250 micron ore was roasted at 850°C for 120 minutes, with the air rate varying from 150 to 210 lph. Increasing the flow rate from 150 lph to 180 lph gave a significant increase from 45.5% to 58.7%, but a further air rate increase to 210 lph only gave a further conversion increase of 0.7%.

The 125-250 micron ore was roasted at 850°C and an air flow rate of 180 lph for periods up to 180 minutes. The vanadium conversion was 47.8% at 60 minutes, increasing to 58.71% at 120 minutes. At 180 minutes, a further increase of only 0.16% was realized.

The effect of ore/salt ratio was tested by roasting 125-250 micron ore at 850°C at an air flow rate of 180 lph for 120 minutes. The Ore/Salt ratio was varied from 25/1 to 25/4. The results are shown in Table V.

TABLE V

Effect of Ore/Salt Ratio on Conversion

Ore/Salt Ratio	Conversion
25/1	22.48%
25/2	30.57%
25/3	58.71%
25/4	50.36%

Apparently, the reason for the decrease in conversion from 25/3 to 25/4 was due to excessive sintering.

Other interesting observations included: A degree of entrainment of not more than 10 %. Some of the salt was volatized and carried off into the effluent. Some sinter was formed at the side walls, the conversion of vanadium was identical in both the sintered and unsintered masses.

2. Thermal Plasma Technology

2.1 Introduction

The term "plasma" refers to a partially ionized gas which is essentially composed of ions, electrons, and neutral species. Overall, plasmas are always neutral since the number of negative charge carriers is equal to the number of positive charge carriers. A plasma is generated whenever sufficient energy is imparted on the gas to cause at least partial ionization.

2.2 Characteristics of Plasmas

Plasma is referred to as the fourth state of matter because of its unique properties. Normally, gases do not contain appreciable numbers of free electrons or ions, and thus act as insulators. However, when a sufficient potential is applied in the gas between two electrodes, the gas becomes ionized. Because of the free changes present, plasmas are electrically conductive and follow the laws of electromagnetism. The electrons are the chief agents for transferring energy from the electric field to the gas. Elastic electron-molecule collisions result in an increase in the kinetic energy of the molecules, whereas inelastic electron-molecule collisions lead to excitation, fragmentation or ionization of the molecule.(30,35)

Plasmas are classified as cold and hot (or thermal) plasmas. Cold plasmas occur under reduced pressures (such as in fluorescent lamps and glow discharges), whereas hot plasmas are formed at atmospheric or elevated pressures (such as in plasma spray torches). Temperatures within hot plasmas can vary from 2,500 to 30,000 K. The electrons will generally be around 100,000 K while the other particles (forming the bulk of the plasma) will generally be in the 10,000 K range.(2,35)

The choice of a suitable plasma gas is very important. The gas can be part of the reaction or serve as an inert carrier. They are chosen to suit the desired industrial process: They may be neutral (Argon, helium, nitrogen), reducing (carbon monoxide, hydrogen, methane), or oxidizing (oxygen, steam) and even such aggressive gases as chlorine have been used. Often, a mixture of gases is used, a small amount of an inert or reducing gas to protect the plasma torch electrodes is used. Recent findings indicate very small additions of certain gases may significantly decrease electrode erosion. The properties of some plasma gases are given in Table VI. In Figure 2-1, it can be seen that the ionization and dissociation of the gas directly influence the temperature achieved . The plasma temperature is plotted as a function of gas energy for several common plasma gases in Figure 2-2.(10,22,26,28)

TABLE VI

Properties of Plasma Gases

Gas	Dissociation Energy kCal/gmole	Particle after Dissociation	Ionization Voltage	Open Arc Voltage	Arc Temp °F	Heat Content of Gas W/ft^3
Ar	0	Ar	15.68	18	18,000	75
He	0	He	24.46	26	27,000	110
H_2	104	H	13.53	70	15,000	260
O_2	110	O	13.55	40	16,000	425
N_2	225	N	14.48	40	16,000	425
Air	--	--	--	60	16,000	425

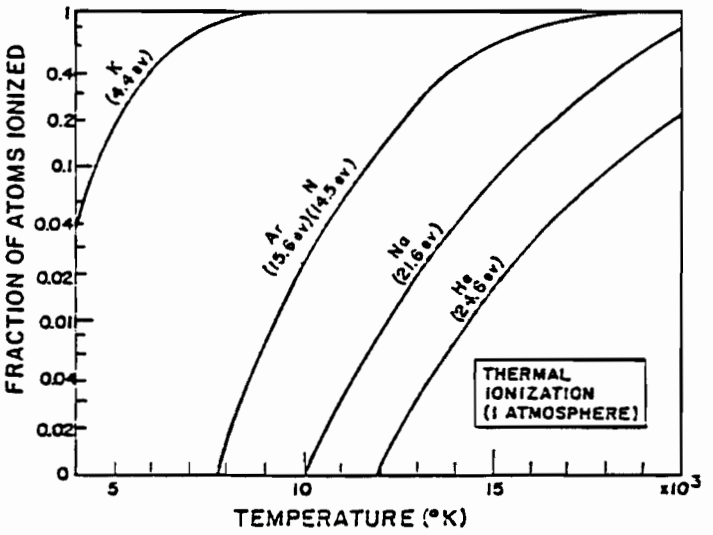

Figure 2-1 - Gas Ionization and Disscociation vs. Temperature [26]

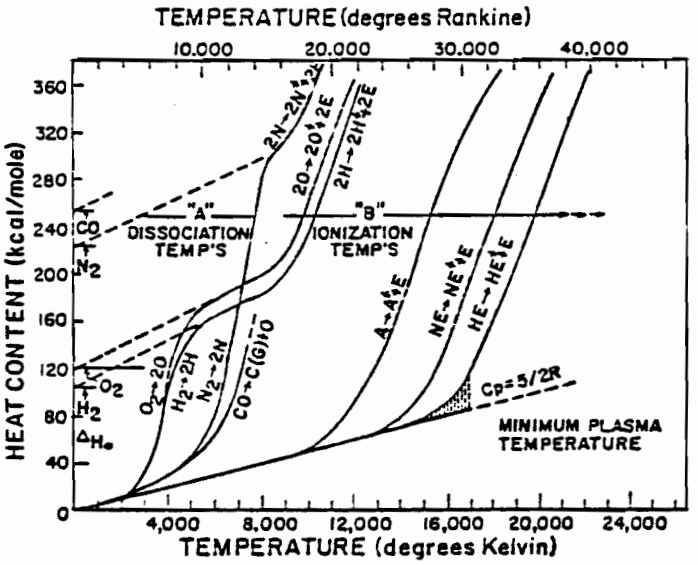

Figure 2-2 - Gas Energy vs. Plasma Temperature[26]

2.3 Plasma Generating Devices

Plasma generators are classified as electrode or electrodeless devices. Electrode plasma generators always have a cathode and an anode, though these may alternate. Such generators can be further subclassified as transferred and non-transferred arc plasma devices.

2.3.1 Electrodeless Devices

Electrodeless plasma generators are less common than electrode generators due to their lower thermal efficiencies, high cost and difficulties in scaling up from laboratory units. The plasma is generated within a water-cooled quartz tube by a high frequency electromagnetic field. Since there are no electrodes electrodeless devices enjoy the advantage of being able to handle corrosive gases such as chlorine, oxygen, hydrogen and vapours of reactive substances.(16)

2.3.2 Electrode Devices

In a non-transferred arc plasma generator, the cathode is placed close to the anode. An arc is struck between the two electrodes and the plasma gas is formed which then emerges from a

nozzle as a jet. The length of the arc is usually in the range 1-5 mm and it is the region of highest temperature in the torch. However, the jet region is normally used in applications due to the small volume and short residence times attainable within the arc zone. The arc is ignited by striking a low current between the cathode and the nozzle or by striking a high frequency arc between the electrodes.(8)

A transferred arc plasma generator differs by its placement of the electrodes. The anode is placed away from the cathode and can take different forms, such as a molten metal bath or a metal piece in the case of metal cutting. Transferred arcs usually range from a few centimeters to tens of centimeters in length. The longer arc provides longer residence times for gas and particulate treatment.(3,8)

When choosing the material of the electrodes, three basic choices can be considered: graphite, tungsten and copper. Graphite requires no cooling, but is consumed during operation, providing a source of contamination. Tungsten and copper electrodes must be water-cooled but are not consumed. For most applications, these two materials are the most popular.(14)

Although many plasma jets have been perfected for various uses in industry and research, the most common type for all sorts

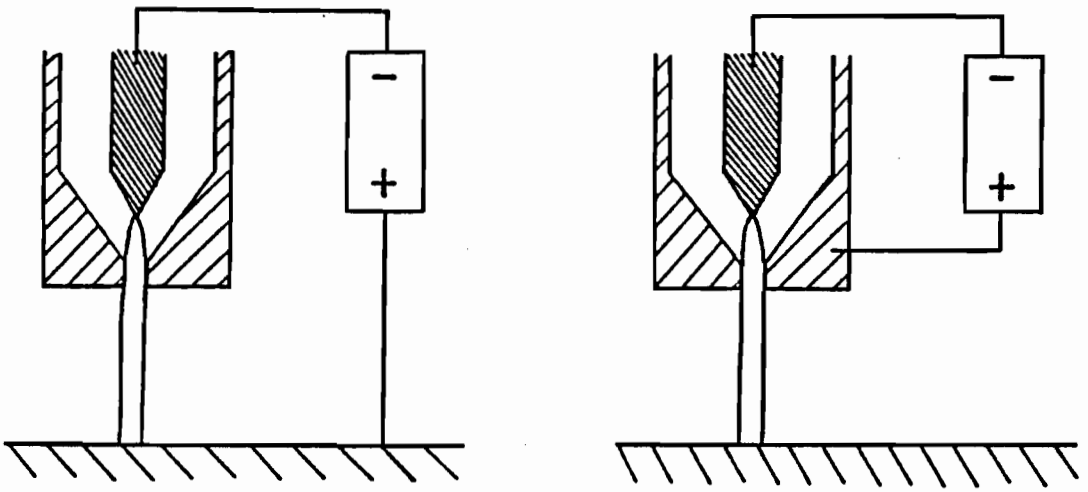

Transferred-Arc Operation

Conventional D.C. Operation

Figure 2-3 - Various Modes of Operating a Plasma Torch

of chemical processes is the direct-current gas-stabilized plasma arc, shown in Figure 2-4.(10)

2.4 Applications of Thermal Plasmas

2.4.1 Introduction

Though the concept of applied plasma may seem new to some, the first known plasma experiment was conducted in 1797 by Henry and Dalton, making acetylene from methane in a capacitive discharge. Progress was slow since then until the invention of the high-frequency torch in 1948 and the d.c. arc torch in 1957. The development and application of plasmas for high temperature physical and chemical processes boomed in the seventies due to improved diagnostic techniques and the oil shock. The oil shock and its associated effects resulted in a favoring of non-fossil fuel dependant processes. Plasma processes use electricity which can often be produced from sources other than fossil fuels.(11, 26,34)

2.4.2 Incentives to Development

Generally there are three main incentives to further development of plasma technology. First of all, it has become apparent in recent years, particularly in more-developed coun-

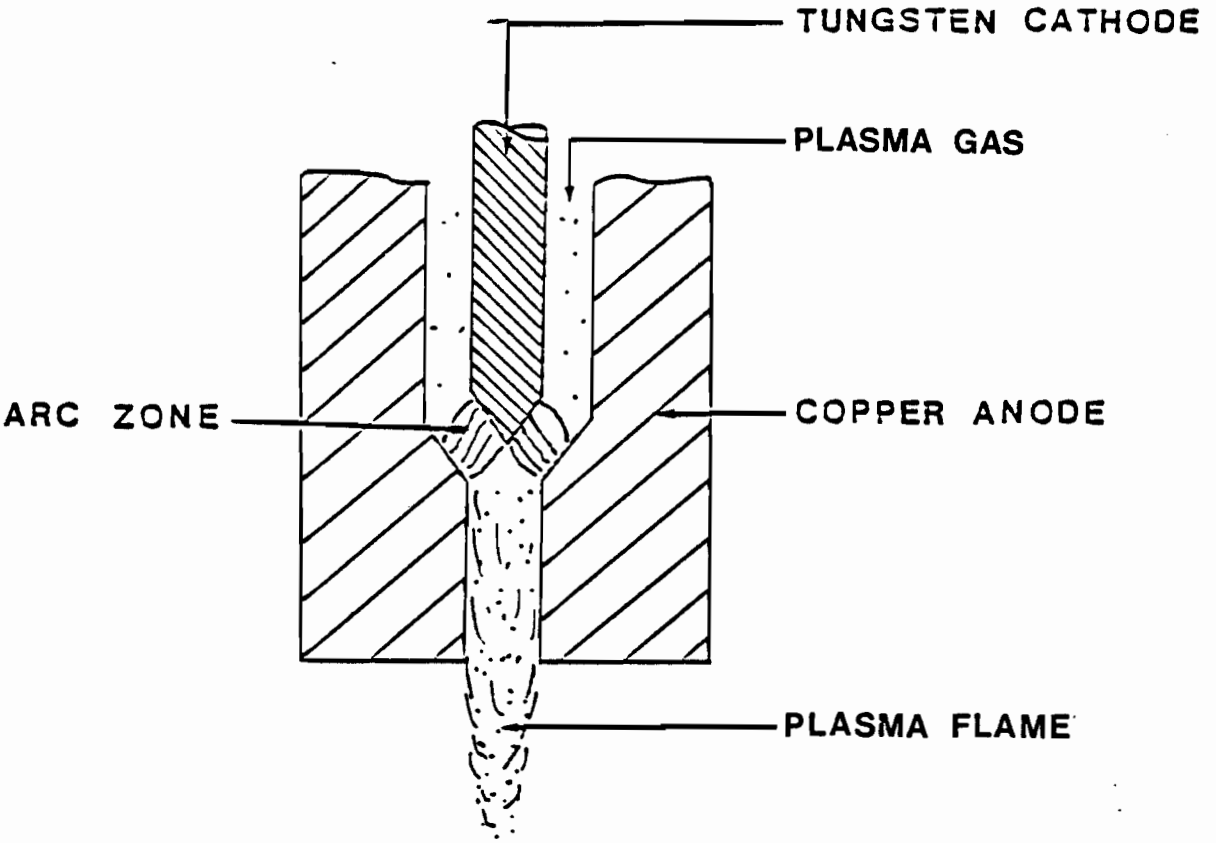

Figure 2-4 - Direct-Current Gas-stabilized Plasma Torch

tries, that the continued use of oil and natural gas as the principal sources of energy is a doubtful proposition. As these societies are moving towards economies based on electrical power, more emphasis is being put on other resources (such as coal and uranium), and the development of new technologies (such as fast breeder reactors and nuclear fusion). As a result, there are strong incentives to develop electro-intensive chemical processes. To illustrate this point, one may compare the use of plasma with natural gas. Assuming a theoretical flame temperature of 1970°C (3560°F) for the combustion of natural gas, the combustion products have an enthalpy of only 720 kcal/kg (1300 Btu/lb). Furthermore, only a limited portion of this energy is made available. By comparison, the plasma arc heater can heat air at 2220 kcal/kg (4000 Btu/lb) and make most of this energy available over a wide range of temperatures. Secondly, in the fields of mineralurgy and extractive metallurgy, there exists a growing need for improving the value of new primary materials. Primarily, this is due to the scarcity or unavailability of certain raw materials. Plasma technology lends itself as one of several alternative routes warranting further technological research. Finally, from an ecological viewpoint, plasma systems produce fewer kinds of, and smaller quantities of pollutants. Generally, depending on the particular process, they produce only carbon monoxide, hydrogen and small amounts of carbon dioxide and water vapor.(5,10,38)

The very high gas temperatures (>10,000 K) measured in arcs and plasma jets make them most suitable for processing inorganic materials and organic compounds of very simple structures. In particular, plasma reactors are well-suited for endothermic reaction systems in which the reaction products are stable at high temperatures. Processes include reduction of sulphides, separation of mineral oxides, reduction of oxides, and conversion of volatile chlorides to metals (by thermal decomposition). Additional advantages include: rapid reaction rates, smaller apparatus, continuous rather than batch processing, easy integration of automated control, and useful new products.(8,10,23,36)

The applications of thermal plasmas can be classified into three categories: Mechanical processes (such as welding, cutting, spraying and spheroidization), metallurgical processes (such as metal extraction from ores, alloy production and the production of refractory materials), and chemical processes (such as for the synthesis of products such as nitrogen oxides, acetylene, phosphates and halogen borides).(8,30)

2.4.3 Mechanical Applications

Mechanical processes using plasma technology are fairly common and well proven. High energy densities in the arc result

in high efficiencies and fast rates of welding and cutting. The main problems encountered are the electrode life and the possible production of toxic vapors, depending on the materials used. Plasma spraying and spheroidization are also commercially proven mechanical processes. In plasma spraying, materials are injected into the arc as powders and are sprayed onto a surface as a coating at high speed (> 100 m/s) and high temperature (4,000 K - 15,000 K). The principal applications of spheroidization processes are in making solid ink, abrasives, catalysts and materials with controlled porosity.(8,10)

2.4.4 Metals Processing

Plasma technology has become common in various metals processing applications. Processes include the melting, refining and alloying of metals. The advantage of using plasmas in the reduction of mineral concentrates is largely due to the improved reduction kinetics and thermodynamics available to effect the required reduction reactions at the elevated temperatures achieved through plasma. It must however, be mentioned that these kinetics and the different stages of the chemical reactions are for the most part, not well known, or unknown. Bethlehem Steel, U.S.A., has developed a process to reduce iron ore to iron in a single step in its 1 mW pilot plant. A schematic is shown in Figure 5-5.(26,30)

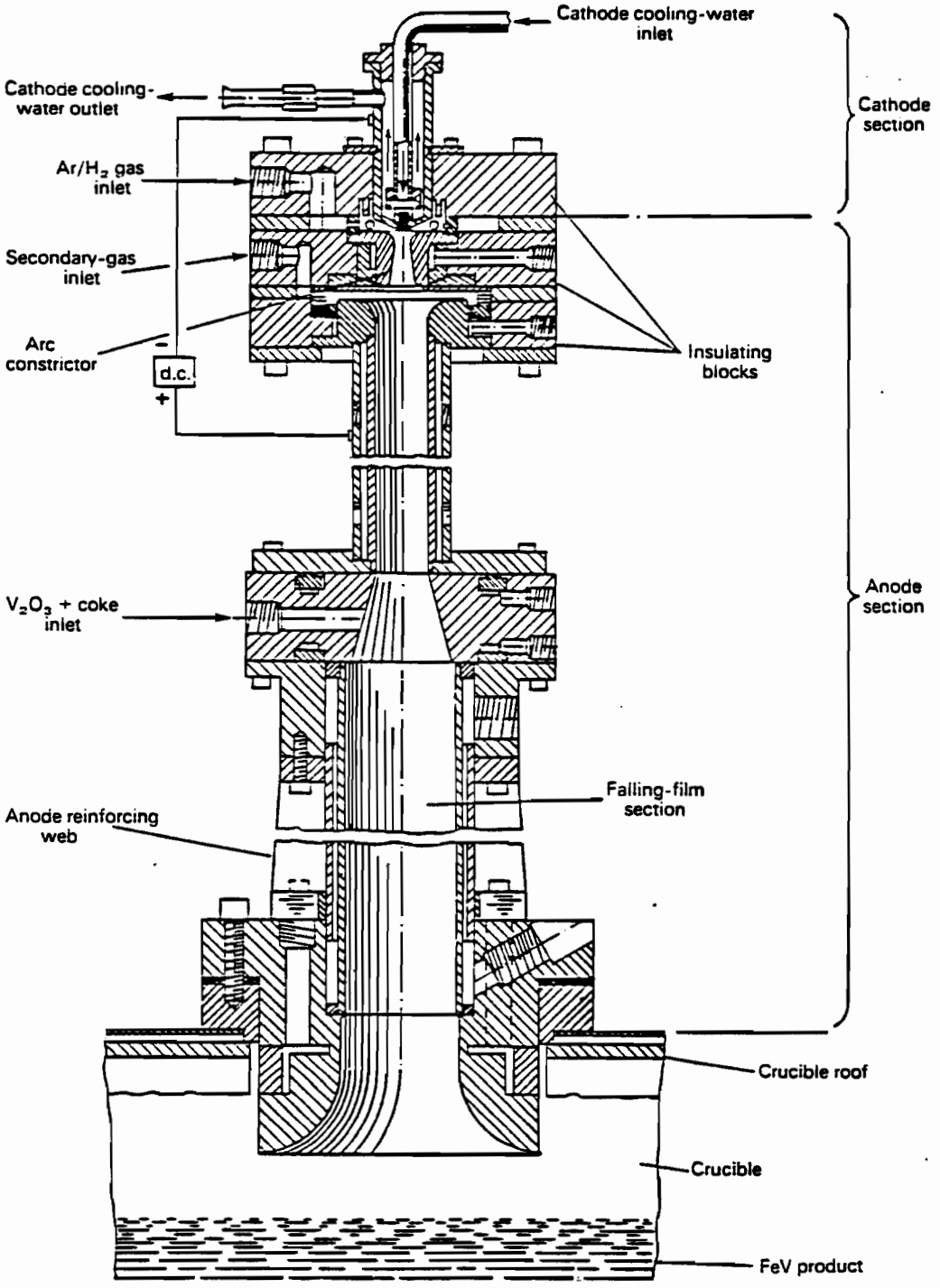

Figure 2-5 - Bethlehem Steel Plasma Furnace[30]

2.4.5 Chemical Processing

Finally, the most important application of plasma technology in chemical processing is the production of acetylene (an important intermediate for plastics, paints, vinyls, aerosols and other products). Other plasma chemical processes are still in their experimental stages. They include the production of boron from its halides (Union Carbide, U.S.A.), nitrogen oxides from N_2 and O_2 (Germantown Labs, U.S.A.) and the production of acetylene from coal (AVCO, U.S.A.).(30,31)

3. Spouted Beds

3.1 Introduction

The term "spouted bed" was coined at the National Research Council of Canada in 1954 by Gishler and Mathur. The technology was originally developed as a method for drying wheat. It was found that much hotter air could be used without damaging the grain. The concepts developed were soon found to be applicable in various processes using different materials.

A spouted bed consists of a vessel of cylindrical or conical shape. The vessel is packed with relatively coarse particles. A fluid is injected at the bottom of the vessel through a small control hole. If the fluid velocity is high enough, a stream of particles will rise rapidly up within a hollowed central core, (called the spout) in the bed of particles. As they fly above the top of the bed, they fall down the sides back onto the bed. Perpetrating a cyclical motion they slowly sink down the sides of the bed (called the annulus), and to some extent to the center of the bed where they are reentrained. Cylindrical vessels with conical bottoms are most common, though purely conical vessels are also used.(40)

Spouting can be achieved with liquids as well as with gases. However, the advantages that spouted beds have over fluidized beds are eliminated when using liquids, thus gases (usually air) are used almost exclusively.(40)

3.2 Characteristics of Spouted Beds

Originally, the spouted bed was conceived as a modified version of a fluidized bed, and is still often referred to as such. However, research over the years has shown that although spouted beds have certain similarities with conventional fluidized beds, they are also very distinct with respect to their characteristics.

With increasing gas velocity, a bed goes from a static bed, to a spouted, to a bubbling, and finally to a slugging bed, as shown in Figure 2-6. Fluidization is optimized in a spouting bed and of poor quality in a bubbling or slugging bed.(40)

3.2.1 Spouting depth and maximum spouting velocity

A typical spouted bed usually has a depth of at least one column diameter. Operating spouted beds at shallower depths is possible, but the hydrodynamics change substantially. As a result, generally formulated principles of spouted bed behaviour

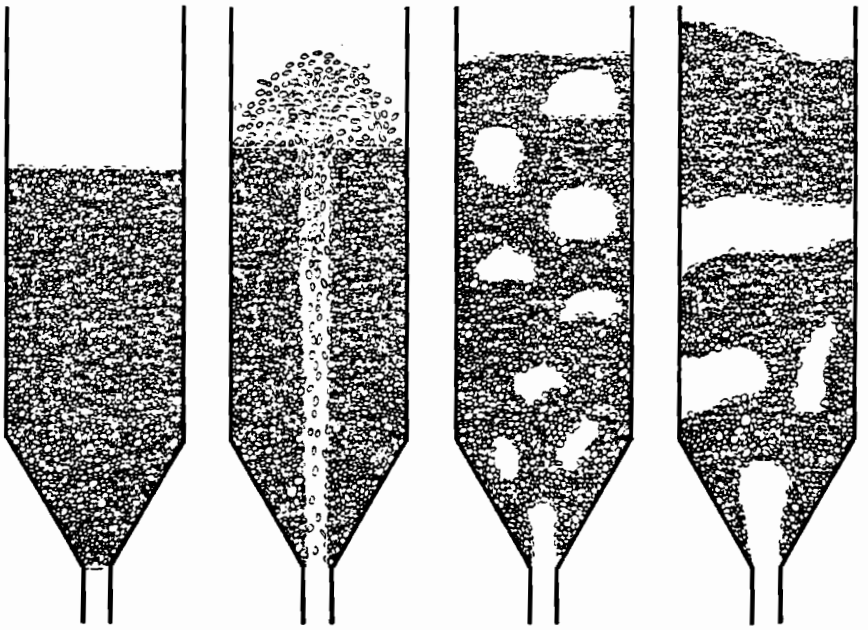

Figure 2-6 - Four Stages in a Spouted Bed[31]

do no longer apply. A minimum spoutable bed, as well as a maximum spouting velocity has not been precisely investigated. Generally though, there is ample latitude between the minimum and maximum spouting velocity so that the velocity can be increased by a large factor without transition to fluidization.(40)

3.2.2 Minimum spouting velocity

Though the minimum spouting velocity is of rather academic importance in most practical cases, it nevertheless provides a guideline to variations in the gas flow rate. Over the years, the Mathur-Gishler equation has proven to be valid over a wide range of conditions.(40)

$$U_{ms}=(d_p/D_c)(D_i/D_c)^{1/3}(2gH(p_s-p_f)/p_f)^{\frac{1}{2}}$$

where U_{ms} = minimum spouting velocity
d_p = particle diameter
D_c = column diameter
D_i = fluid inlet diameter
H = bed depth
p_s = particle density
p_f = fluid density
g = acceleration of gravity

3.2.3 Spouting Stability

The regime of a stably operating spouted bed is critically dependant on several conditions. Unless these are satisfied, the

movement of the particle becomes random, and spouting passes to aggregative, bubbling fluidization.

Among several conditions to be satisfied concerning the bed geometry, the most crucial are the orifice to column ratio, the cone angle, and the inlet design. Generally, a ratio of 0.35 applies for a satisfactory orifice to column ratio, however, this ratio decreases considerably for small particles. The cone angle is strongly dependant on the internal friction characteristics of the particles, but for most materials the limiting cone angle seems to be around 40°. Several improvements have been made on inlet designs. Among some findings: spouting is improved with a inlet orifice somewhat smaller than the narrow end of the cone. Also, improvements, especially with finer material were experienced with inlets protruding slightly into the bed.(40)

Generally, a minimum particle size for spouted bed operation is 1 mm. However, it has been shown that satisfactory spouting can be achieved with much finer particles, as long as the gas inlet diameter does not exceed 30 times the particle diameter. Less organized spouting can be possibly achieved without adhering to this condition. A uniform particle size distribution favors good spouting. Generally, size distributions of a factor of 5 can be satisfactorily spouted.(40)

In shallow beds, it has been found that an increase in gas flow much above the bed surface causes the spout above the surface to lose its shape, and though the movement of particles above the bed becomes chaotic, the regular downward motion of particles in the annulus remains intact. In deeper beds, slugging becomes a problem with increased gas flow rates.(40)

3.3 Applications of Spouted Beds

3.3.1 Conventional Applications

With development over the years, the spouted bed has found its use in a variety of applications. Primarily, a spouted bed is useful for drying, heating, and cooling of granular solids. In coating and granulation, the spouted bed has an advantage in that the particles are in a regular cyclic motion, allowing enough residence time in the annulus between depositions for each layer to dry until the next one is deposited in the spout. Attrition commonly encountered in spouted beds, plays a key role in various applications including coal carbonization, shale pyrolysis, and iron ore reduction. Other conventional applications are found in thermal cracking of petroleum and charcoal activation.(40)

3.3.2 Plasma Spouted Beds

Preliminary research into plasma spouted beds has been conducted at the Université de Sherbrooke (Québec). Argon, and argon/nitrogen plasmas were used in fluidizing and heating alumina powder beds. A diagram of the Sherbrooke reactor is shown in Figure 5-7.(20)

The experiments were conducted with alumina powder of different particle size ranging from 53 m to 1000 m. The power was varied from 9.0 to 28.0 kW. The plasma torch was operated with either pure argon at 47 l/min or an argon/nitrogen mixture at 37.3 l/min, with 38% N_2 by volume. Various factors such as bed stability (the definition of a stable bed is a bed that does not melt, fuse or altogether disappear), temperature profiles, particle size changes, and particle recirculation were investigated.(20)

At lower particle loadings, the plasma core was visible at the bed surface. At higher bed loadings, the plasma core was completely immersed in the bed. The bed, however, remained well fluidized with a high rate of powder recirculation. At the highest bed loadings, the bed became increasingly unstable with visible bubbling and slugging. Unfortunately, the effect of dp, the mean particle diameter on bed stability was not reported.

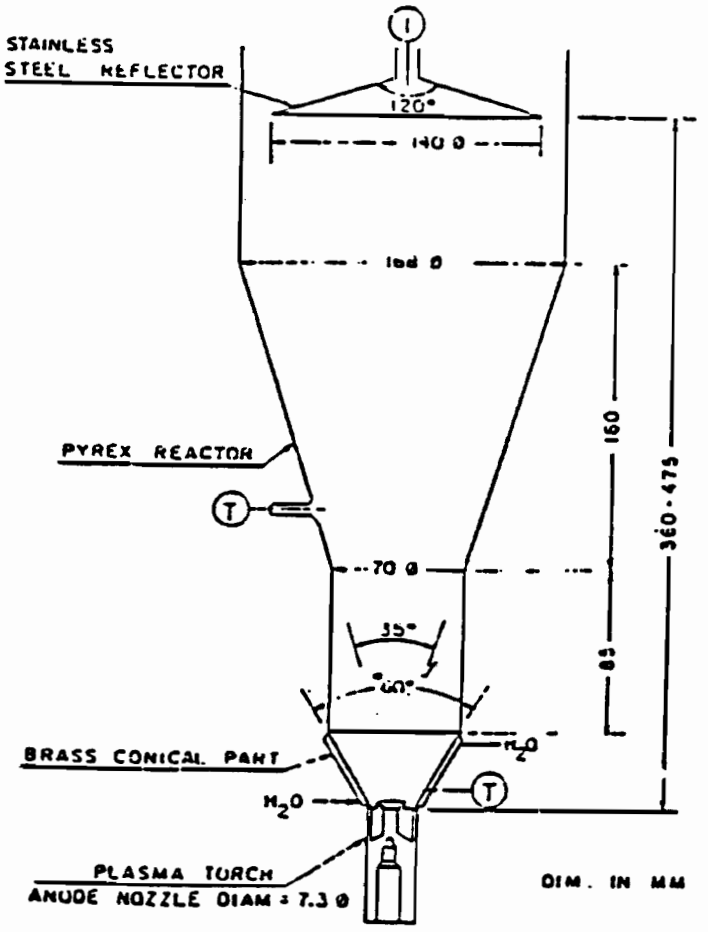

Figure 2-7 - Sherbrooke Plasma Spouted Bed Reactor[20]

Generally, larger particles provide for more stability than smaller particles.(22)

Due to the high level of particle recirculation in the bed, the entire unit is at a reasonably uniform temperature. The temperatures ranged as high as 1143 K, but were generally in the 900 to 1000 K range.(20)

Analysis of the particle size distributions, before and after the runs, showed a significant decrease in the average particle size. This has been attributed to either particle-particle or particle-deflector (a deflector plate is fixed above the bed to prevent excessive particle entrainment) collision, or simply thermal shock of the particles as they are exposed to extremely high temperatures when passing through the plasma flame.(20)

4. Conclusions

The literature review has shown that whereas the various components of the proposed process have been studied to certain extents, the process as a whole constitutes an unknown field.

The metal vanadium is of importance in various technologies. In particular, the aerospace and tools industry has a constant demand of vanadium. The vanadium ore mining and production industry is concentrated in a few sites around the world including the U.S., Soviet Union and South Africa. Several processes are used to extract the vanadium from vanadium-containing ore. The most popular is the salt roasting and water leaching technique. The effects of the variables affecting the efficiency of this technique has been covered in several articles. Though explanations are often lacking, recommendations among the various articles are usually complete and consistent.

Over the past few decades, thermal plasma technology has found an increased range of applications. By no means minor is its adaptibility to various processes in metallurgy. The use of thermal plasmas entails many advantages including ease of control, small process sizes, relative efficiency, as well as in ecological and economical aspects. The simple operation of thermal plasma devices is well understood, and much research

concentrates on the adapting of thermal plasma technology to various existing and new processes.

The operation of spouted beds has been studied extensively, though many aspects claim for additional investigation. In particular, the operation of spouted beds with very small particles is not well understood. Many of the concepts and relationships that hold for large particles fail to provide an accurate account for smaller particles. It appears that though spouting of small particles is possible (usually with higher flow rates), its quality is inferior to that of larger particle spouting.

CHAPTER III

EQUIPMENT

1. Supplies

1.1 Plasma Gas & Air

The operation of the equipment entails the need for supplies of nitrogen and argon for the plasma torch, and of air for the reactor. Industrial-grade nitrogen and argon are supplied through single cylinders, with pressures regulated to 100 psig with appropriate pressure regulators. Polyvinyl reinforced tubing connects the cylinders to the control console (Metco Type 2MC, see Figure 3-1). Two rotameters on the console are used to regulate the gas flow. A safety feature is incorporated into the console which shuts off all supplies, including the gas flows automatically should the pressure fall below 50 psig, or if the shut-down button is pressed. Due to the procedures adopted for the experiments (see Chapter IV) it is necessary to keep the nitrogen gas flowing even after the shut-down button is pressed. For that purpose, the solenoid valve has been rewired to allow for a manual opening and closing. From the rotameters, the gases flow directly to the torch through a single line. The pressure of the gas in the cylinders is indicated by the pressure regulator dials as well as analog displays on the console.

Air is supplied directly from the laboratory lines. The pressure and flow is regulated with a pressure regulator and

standard rotameter respectively. The air line assembly is shared with another system in the lab, and for that purpose valves have been installed to direct the air flow to the desired system. All lines are of polyvinyl reinforced plastic.

1.2 Power

Power was supplied by a 400 V, 3-stage rectifier and was regulated by a control console manufactured by Metco Incorporated. It was originally intended for use with plasma spraying equipment, but can be adapted to a variety of plasma process applications. To monitor the power both the current and voltage were displayed on analog meters. The power output could be varied continuously by a rheostat. The exact ratio of current to voltage was pre-determined by the type of plasma gas used and other conditions. As a safety feature, the power output could be terminated instantly with a single button.

1.3 Water

City water at a pressure of 100 psig is supplied from the laboratory lines for cooling. Four calibrated rotameters to supply cooling water for the torch, the heat exchanger, the flange and the reactor viewing port. The maximum flows are 32

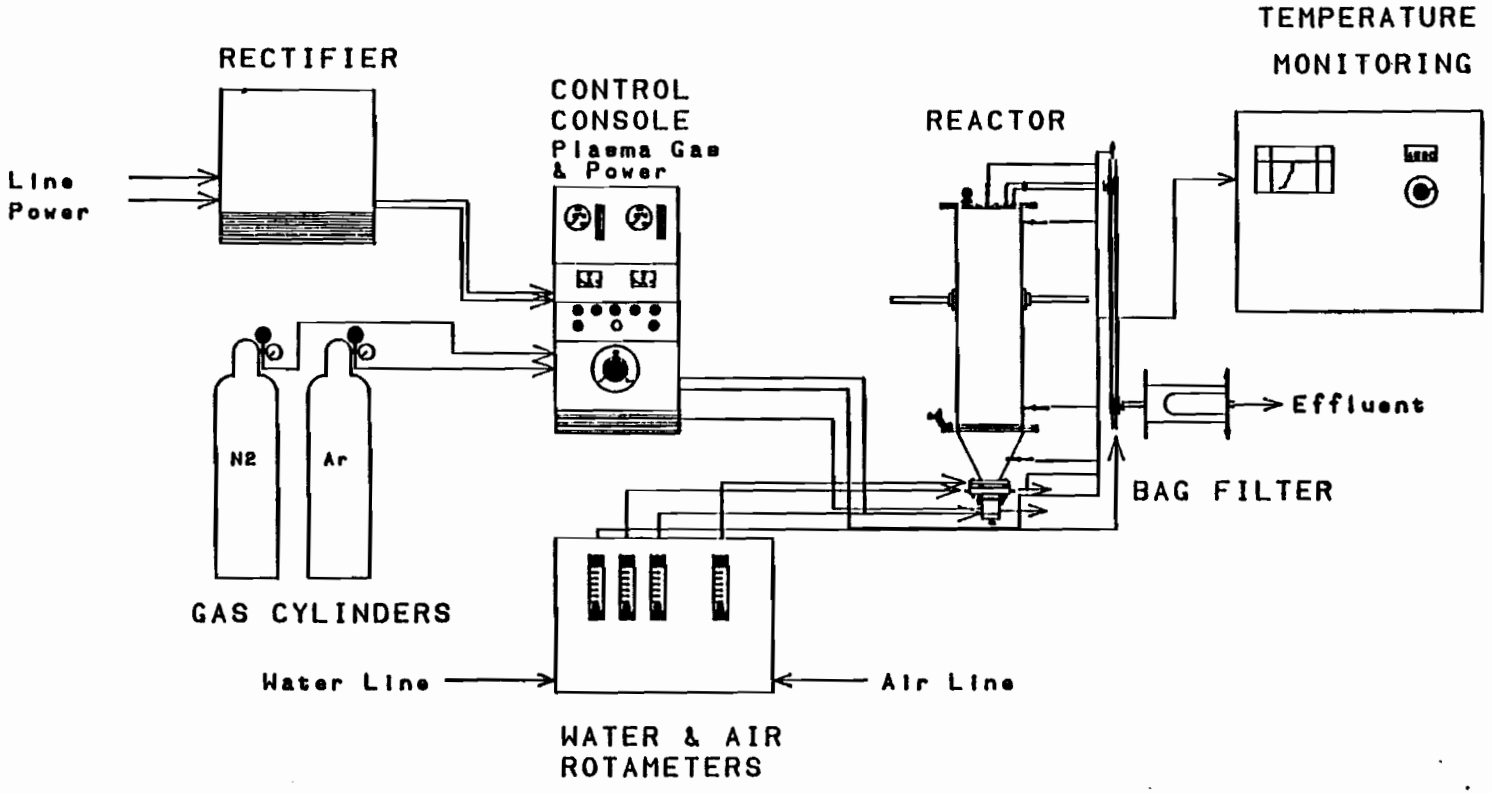

Figure 3-1 - General Equipment Diagram

lpm for the torch, 28 lpm for the torch, 12 lpm for the flange and 2 lpm for the view port. Typical flow rates during experiments are 7 lpm for the torch, 21 lpm for the heat exchanger, 10 lpm for the flange and 2 lpm for the view port. The lines to the rotameters are of carbon steel. The lines from the rotameters to the flange and the view port are of polyvinyl unreinforced tubing, and the lines to the torch and heat exchanger are of polyvinyl reinforced tubing to withstand the higher pressures.

2. Reactor Unit

2.1 Torch

The torch is adapted from a design by M. Boulos of the University of Sherbrooke. It is a non-transferred arc, D.C. plasma torch with specifications given in Table 3-1. A 1:1 scale schematic drawing of the torch is given in Figure 3-2.

2.2 Reactor Shell and Frame

The reactor shell consists of two main parts; a long tubular section and a shorter conical section forming the bed. Both sections are made of Type 304 stainless steel, of which the specifications are given in Table 3-2. The shell and cone components have been used previously in research conducted by Paul Stuart. Though it is recommended that the steel not be heated above 870°C, Stuart frequently used temperatures in excess of this without any deterioration. Two brackets were welded onto the shell to allow it to be suspended on a swivel mount. The complete reactor was suspended in a 3/4" iron tube frame designed to give maximum stability and at the same time allow maximum access to the reactor parts. A schematic drawing of the set-up is given in Figure 3-3.

TABLE VII

Plasma Torch Specifications

Optimum Power Range	:	10 - 20 kW
Optimum Voltage Range	:	30 - 50 V
Optimum Current Range	:	300 - 400 A
Open-Circuit Voltage Requirements	:	140 - 160 V
Cooling Water Flow Rate	:	26 lpm (suggested)
Cooling Water Pressure	:	60 psi (recommended minimum)
Suggested Gas Flow Rates		
Nitrogen	:	30 - 40 lpm (100 lpm max.)
Argon	:	50 lpm

Source: J. Jurewicz, Dept. of Chemical Engineering, University of Sherbrooke, Sherbrooke, Quebec.

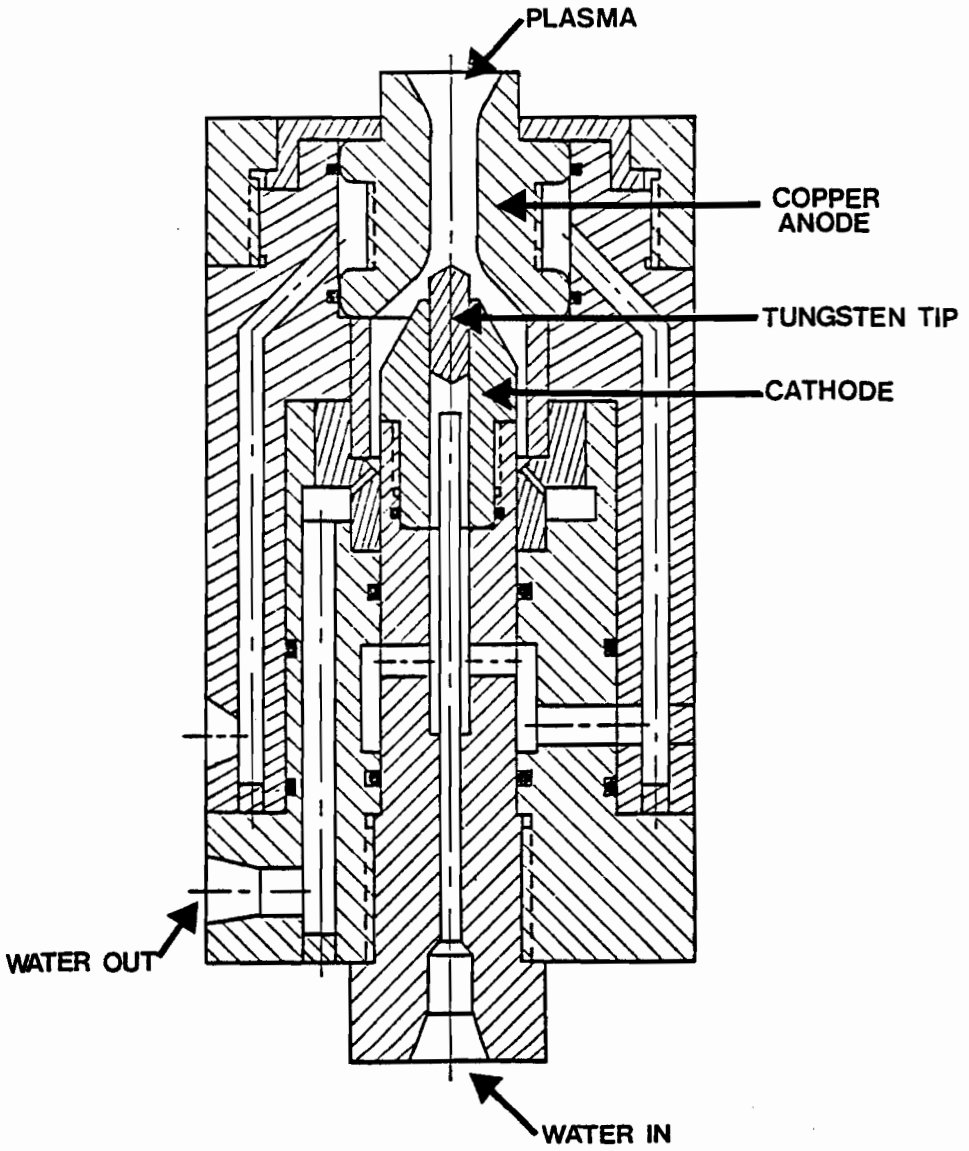

Figure 3-2 - Schematic of Plasma Torch

TABLE VIII

Stainless Steel Type 304 Properties

Melting Range	1400-1455°C
Density	8.03 g/cm^3
Coefficient of Thermal Expansion	16.56 cm/cm/°C (20-100°C)
	19.8 cm/cm/°C (100-870°C)
Maximum Operating Temperature	870°C (intermittent use)
	930°C (continuous use)

Source: Anon., 'Stainless Steel Handbook', Allegheny Ludlum Steel Corporation, 1959.

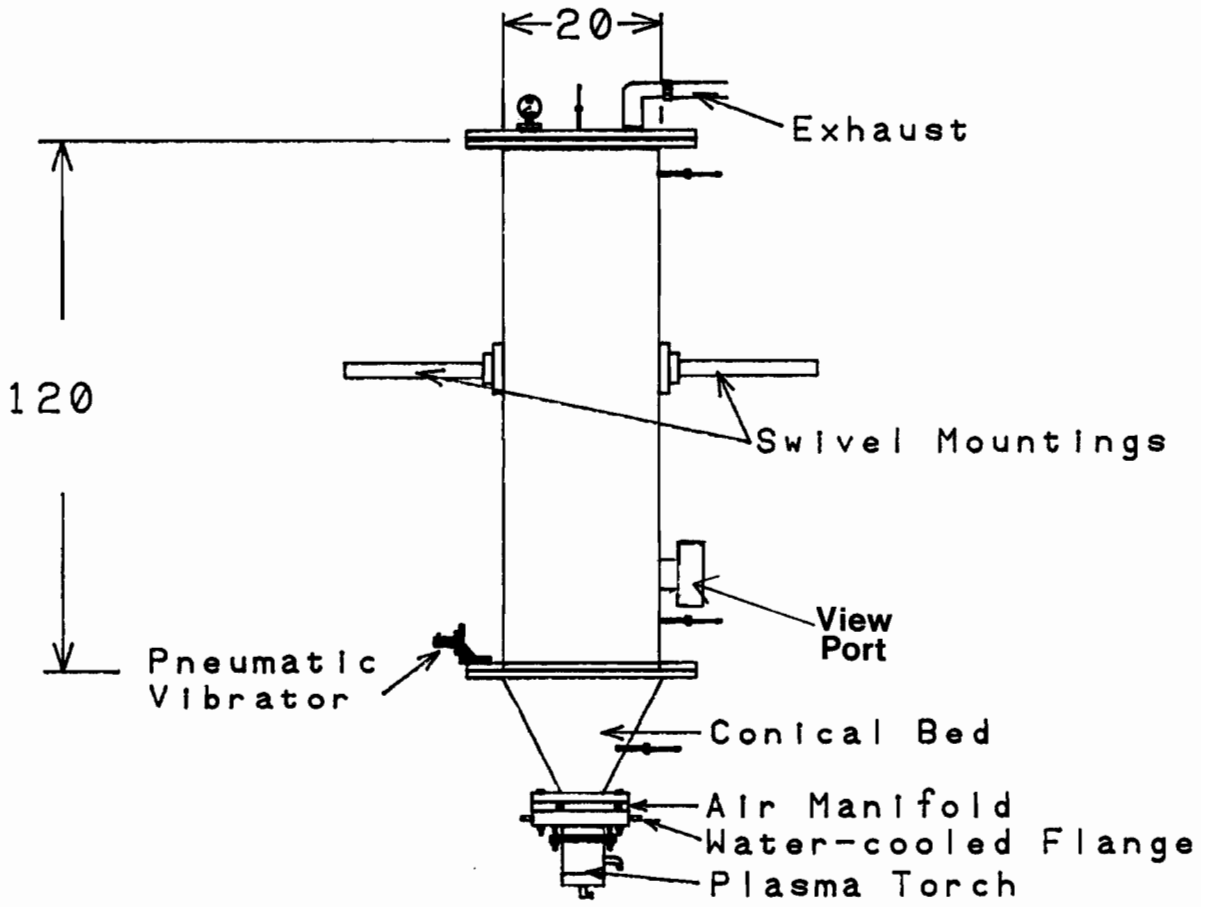

Figure 3-3 - Diagram of Reactor Set-up

A pneumatic vibrator was later attached to the joint between the reactor shell and cone. The purpose of the vibrator was to enhance particle circulation. The vibrator is fed with compressed air from the laboratory lines which is passed through a lubricator.

2.3 Bottom Cone Assembly

The main part of the reactor is the bottom cone assembly containing the torch, water-cooled flange, air manifold and particle bed (cone). A scaled schematic drawing of the assembly is given in Figure 3-4. The four parts are arranged in the following order; cone, air mainfold, flange, and torch. The air manifold and flange are connected to the cone by six bolts and are separated by two high-temperature gaskets. The faces of the cone, manifold and flange are all 'phonogram'-finished to avoid leaks at the gaskets. All parts except the torch are constructed of stainless steel.

The manifold has six air inlet passages. Three are oriented tangentially, whereas the other three are oriented radially. Only one orientation can be chosen at any one time. For most applications, the tangential orientation was optimal. The passages were sized to 0.635 mm diameter (0.25 in.) as an

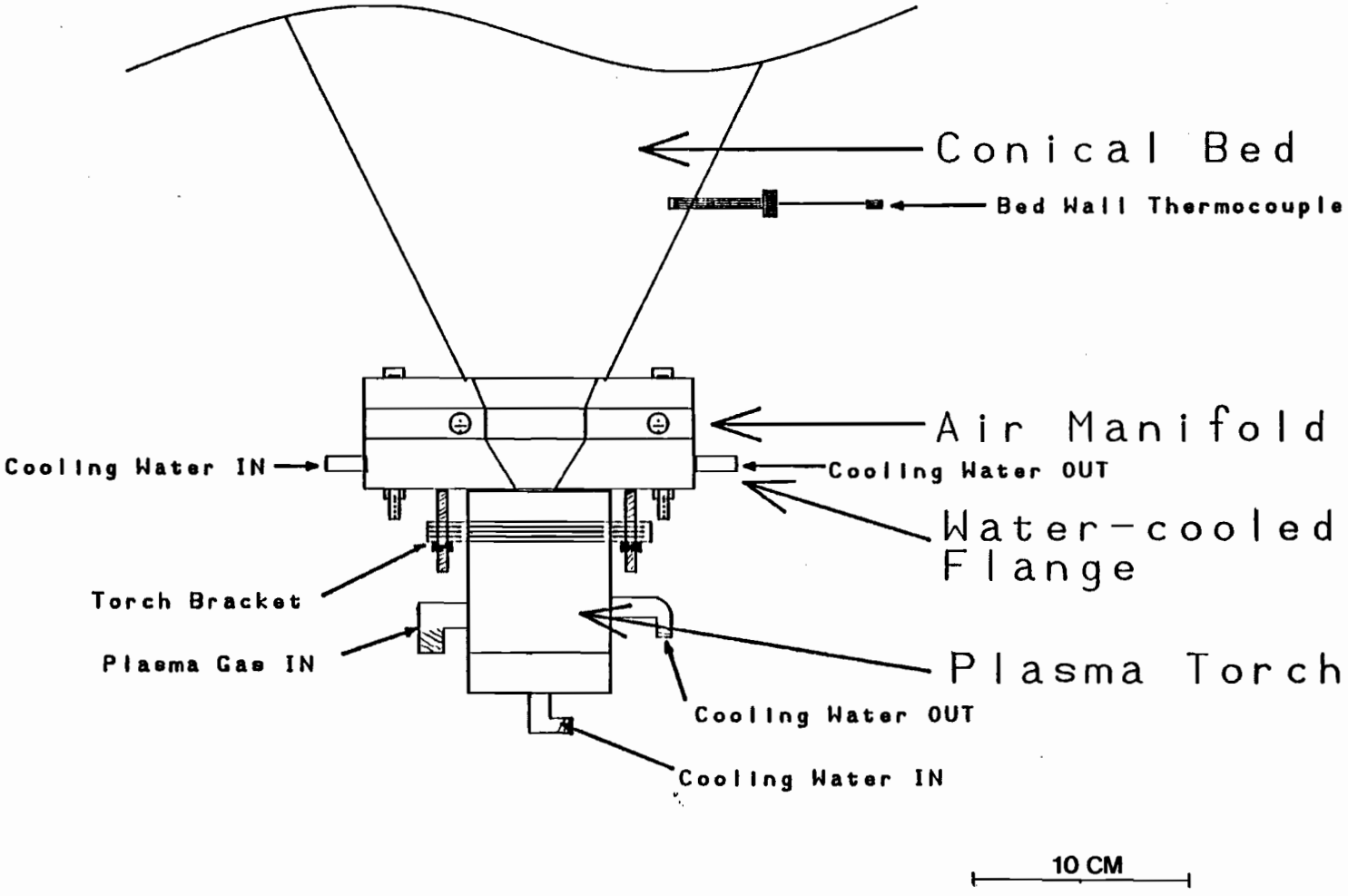

Figure 3-4 - Bottom Cone Assembly

acceptable compromise between an adequate maximum air flow and minimum decrease of structural strength.

The flange was necessary to minimize heat transfer by conduction from the other components to the torch . It is made of 0.635 mm thick (0.25 in.) stainless steel and is water-cooled. The water enters near the bottom, and exits near the top at the opposite side, minimizing areas of poor circulation as well as air bubble build-up. The inside conical cut-out of the flange was later supplemented with a boron nitrite insert due to arcing problems (arcs would extend from the torch, burning holes into the steel cone). Three bolts to attach the torch are screwed into the bottom side of the flange. The torch is sealed to the flange with an o-ring seal.

2.4 Top Cover Assembly

The top cover assembly consists of the cover, a deflector plate with extension pipe fitted for a 1.5 m thermocouple, an exit fitted with a connection to the heat exchanger, and a multi-purpose port. The port was originally intended to feed particles, but was finally fit to hold a pressure gauge. The cover is constructed from 0.635 mm thick (0.25 in.) stainless steel and is connected to the reactor upper flange with six bolts. A high-temperature gasket is used for sealing.

The deflector plate is connected to the cover by a two-piece extension tube (allowing for a variation in length). The plate is sized to provide approximately 1 cm of space between itself and the reactor wall. Its purpose is to prevent excessive entrainment of particles by redirecting them back to the bed. A 1.5 m long, 0.635 cm thick (0.25 in.) thermocouple can be fit through the extension tube, deflector plate, and cover. It is fixed by a nylon ferrule swagelok fitting so that its vertical height can be changed. The exhaust exit is fitted with a 2.54 cm (1 in.) brass swagelok joint which connects to the heat exchanger. See Figure 3-3.

3. Auxiliaries

3.1 Heat Exchanger

Before the reactor effluent could be passed through the plexiglass bag filter and then to the main exhaust, it had to be sufficiently cooled. A simple double-pipe heat exchanger was constructed and attached directly to the exhaust fitting on the reactor's top flange. It was thus an integral part of the swiveling assembly.

The heat exchanger consisted of two brass pipes approximately 1 meter long. The inside pipe was 1.27 cm (0.5 in.) in diameter, and the outside pipe was 2.54 cm (1 in.) in diameter. The inside pipe carried the cooling-water, counter-current to the gas flow. The outside pipe carried the effluent gas. This maximized heat transfer since the gas is exposed to both the cold water on the inside, and the relatively cool laboratory enviroment on the outside.

3.2 Bag Filter

After the gas was sufficiently cooled, it was directed to the bag filter. The filter was required for the removal of the

particles for analyses of entrainment and salt losses, as well as for health and enviromental reasons.

The bag filter consisted of a cylindrical clear plexiglas housing 32 cm long, and 14 cm in diameter. The bag was supplied by Porrits & Spenser and was rated for high temperatures and a 100 % collection efficiency to 1 micron. The bag was supported by a wire frame. The effluent was fed to collect the particles on the outside of the bag. This increased the capacity of the filter since a build-up of particles on the bag could be removed by rapping the housing. The filter could be opened easily for removal of collected particles. The cleaned effluent passed directly to a fume hood. See Figure 3-5.

3.3 Instrumentation

Besides the power input and water cooling rates (described in 1.2 & 1.3), the temperatures indicated by the various thermo-couples had to be monitored. Two mechanisms were available. For instant retrieval, a L.E.D. digital display (Thermoelectric) capable of displaying temperatures up to 1700°C was coupled with a rotary thermocouple selector. As a back-up, a didgital mV read-out was also connected.

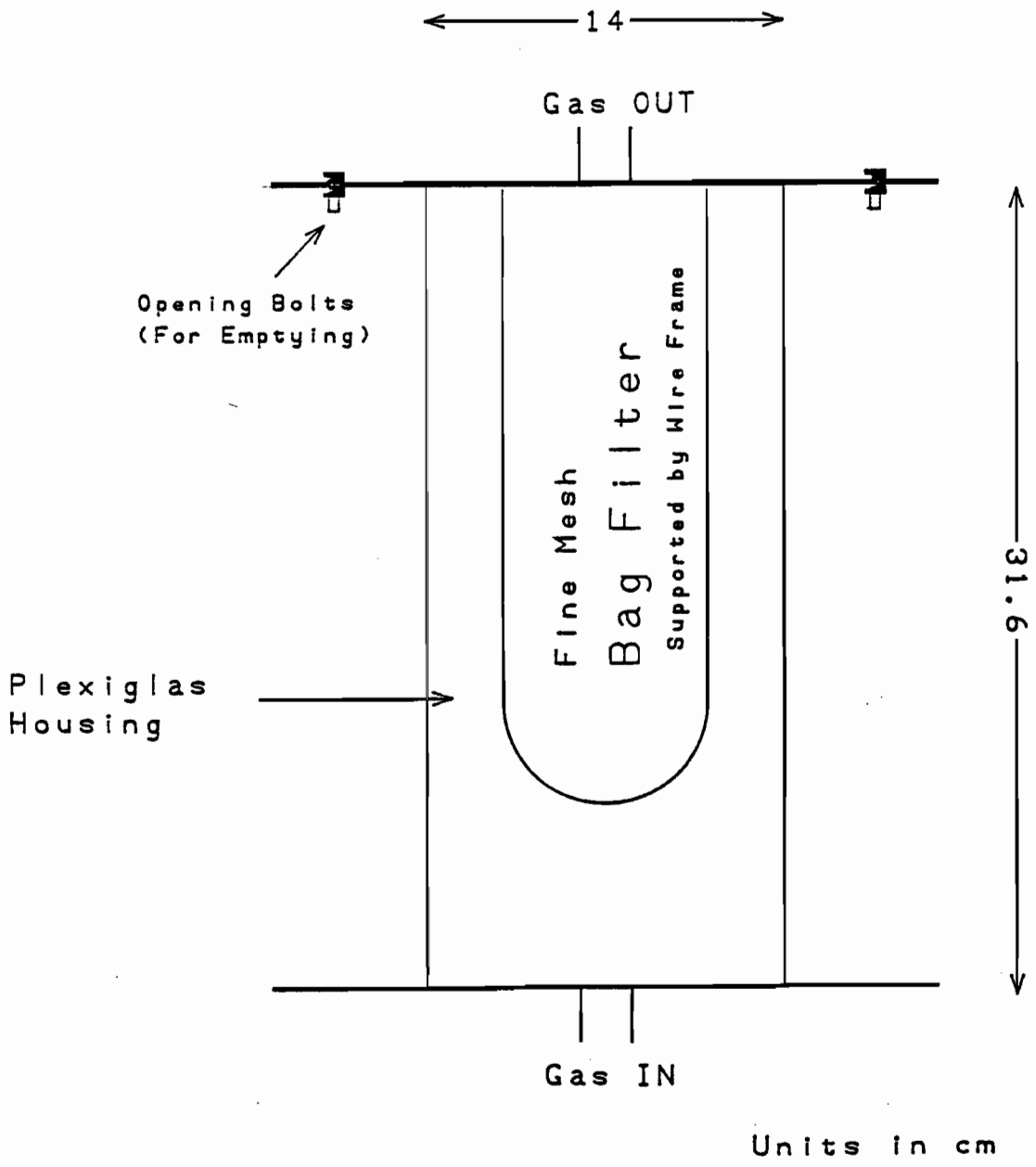

Figure 3-5 - Bag Filter Schematic

A multi-channel strip-chart recorder capable of recording temperatures up to 1200°C was connected for permanent records. Up to four arbitrary temperatures could be recorded for future analysis. For the main experiments, the torch cooling water outlet temperature, and the temperatures of thermocouples #1, #3, and #5 were recorded (see Figure 3-6).

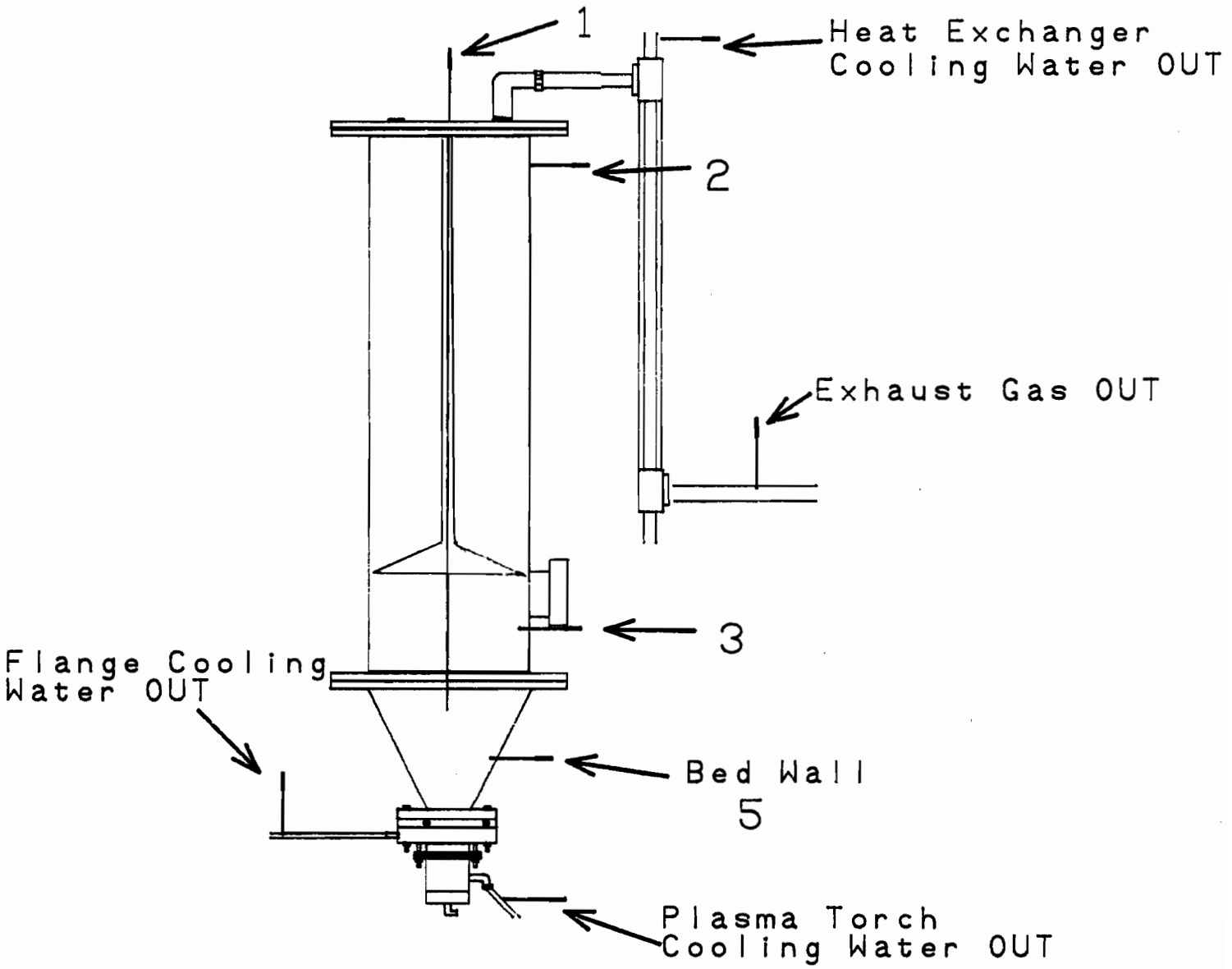

Figure 3-6 - Thermocouple Location Diagram

CHAPTER IV

EXPERIMENTAL PROCEDURES

1. Feed Preparation

For all experiments that were to include reaction studies, it was necessary to add the desired sodium salt. The salt was added in two different ways. The first was to simply mix a prescribed (usually 10%) amount of salt powder physically with the ore particles. This method is fast and simple, but yields poor salt/ore contacting.

An alternative is to add the salt in a simple agglomeration process. A process similar to that of Saha (32) was employed. A measured amount of salt was dissolved in just enough water to give a saturated solution. This solution was then mixed into the ore particles, giving a mud-like texture. Mixing was continued until a visually homogeneous mixture was obtained. Subsequently, with further occasional interruptions for mixing, the material was dried overnight at 110°C. The resulting cake was then hand-broken and sieved to be then used in the reactor. Agglomeration was expected to have two advantages; first, to increase salt-ore contact, and second, to increase the small overall particle size.

Agglomerated and non-agglomerated particles were sometimes sieved to remove excessively fine or coarse particles.

2. Preparation of Equipment

Several steps were completed to prepare the equipment for an experimental run. First of all, the reactor was swiveled into its horizontal position. The heat exchanger and the top cover-deflector plate assembly were then removed to gain access to the inside of the reactor. The prepared particles were subsequently placed inside the reactor, near the bottom on one side of the cone. The heat exchanger and the top cover-deflector plate assembly were then re-attached.

With the particles loaded, a complete checklist was followed to ensure safety. A copy of the actual checklist is shown in Appendix A.

The following major points were checked: The proper connections of the electrical cables from the control console to the torch; ensuring that the cables were not in contact, and at least several centimeters apart everywhere (to avoid the possibility of high frequency arcing across the cables); ensuring that the apparatus was safely grounded; also, both the gas and water lines were regularly checked for leaks.

3. Run Procedures

3.1 Torch start-up

A list of procedures was gone through to start each run. The following steps were considered essential:

Verify Checklist.
Make sure that cooling water flows are on.
Turn on temperature strip-chart recorder.
Adjust plasma gas pressure to 100 psig.
Switch on main power switch (on wall).
Switch on control console, verify that blue 'OK' light turns on.
Turn off all secondary electrical appliances (e.g. thermocouple read-out).
Verify that current rheostat is set to '0'.
Perform High Frequency test with 'HF TEST' button.
Activate open circuit voltage (button # 4 on console), and verify that high-voltage state is maintained when button is released.
Turn on gas flow and adjust to desired flow rate (Argon 50 lpm, 88 on rotameter).
Turn on air flow to desired value.
Start torch with 'IGNITION' button (# 5).

Turn on secondary instrumentation.

Gradually add nitrogen to replace argon.

Adjust rheostat to desired current value.

Swivel reactor into vertical position.

3.2 Temperature Monitoring

During a run, temperatures were constantly measured at various points throughout the system. Inside the reactor, four points were monitored; one near the cone wall inside the bed (useful in confirming adequate circulation/temperature distribution), one centrally above or within the bed (variable in height), one approximately 10 cm above the bed, and finally one at the top of the reactor (effluent before heat exchanger). A fifth thermocouple was later added to the outside cone wall to monitor excessive temperatures of the steel. A schematic of the monitored points is given in Figure 3-6.

Outside the reactor, the cooling water outlet flows of the torch, bottom flange, and the heat exchanger were monitored. Finally, the exhaust gas temperature (out of the heat exchanger) was also measured.

The temperatures were read off two L.E.D. displays (one in

°C, one in mV). Crucial temperatures were logged on a strip-chart recorder.

3.3 Power Monitoring

The torch voltage and current were monitored throughout the run and the current adjusted as needed with the rheostat to maintain constant power conditions.

3.4 Bed Stability

The interior of the reactor was monitored through the view port to determine if proper circulation of the bed was maintained, whether the flame shot through the bed on a continuous basis, and whether the flame was diverted to the wall by fused blocks.

3.5 Shut-down

It was important to prevent the flow of particles (melted or not) into the torch as the plasma flame is extinguished. For this reason, the control console's interlock which stops all gas flows upon 'shut-down' has been overridden to allow nitrogen to continue flowing after the shut-down button has been pressed. This kept the torch free from particles.

Once the shut-down button was pressed, the following procedures were observed:

Push 'OFF' button on console.

Switch off main power switch.

Reduce nitrogen flow to minimum necessary for particles to stay suspended.

Swivel reactor into horizontal position.

Turn off gas flows and cylinders.

Turn off water flows after sufficient cooling.

4. Sample Analysis

4.1 Sample Removal and Weighing

After the shut-down procedures were completed and the system was allowed to cool down completely (preferably overnight), the particles were removed. The reactor top with the deflector plate assembly and the torch were removed. If no solid block fused within the bed, it was usually sufficient to swivel the reactor to the vertical and allowing the particles to flow out into a container. If a solid block formed it was necessary to tilt the reactor back to the horizontal to remove the block through the top opening.

The particles were sieved into three components (if applicable); regular particles, fused but free-flowing chips (above 800 microns), and fused solid blocks. The first two components were present in most runs, the latter occasionally.

Finally, the bag filter unit were weighed (the mass of collected powder was obtained by difference with the empty unit) and opened to remove the collected powder.

4.2 Preparation for Atomic Absorption Analysis

Although several analysis techniques were considered, it was decided to use atomic absorption analysis (from here on referred to as AAA). Several steps were necessary to prepare the reacted samples for analysis. First, the particles were crushed to a fine powder in a 'shatterbox' used in the Department of Mining & Metallurgical Engineering. This was necessary to ensure a maximum particle-solvent contact ratio. Secondly, the crushed powder was leached in water at 80-90°C for 1 hour with constant mixing (This method was suggested by several researchers including Dr. Malinsky of the CRM). The resulting mixture was then vaccuum-filtered to separate the sodium metavanadate rich liquor from the remaining non-soluble particles.

4.3 Analysis for Vanadium

To further prepare the solution for AAA, it was necessary to slightly acidify the liquor with nitric acid as well as dilute to put it in the range detectable by AAA. The thus-prepared samples could then be analyzed for their vanadium content. Four samples of known concentrations were used as standards. The concentrations were chosen to bracket the minimum and maximum theoretical conversion rates. All samples were done in duplicate.

4.4 Analysis for Sodium

To have an estimate of the salt losses encountered it was necessary to measure the salt content in the entrained material as well as in the remaining particles in the reactor. A method similar to the analysis for vanadium was used. The leached liquor was used and diluted to give an expected salt concentration within the detection range of the AAA machine. Again, four standards were used as with vanadium.

CHAPTER V

RESULTS

The results of the work are divided into two main sections. First, the results of preliminary calculations and experiments will be presented. These include such topics as particle size analyses, fluidization curves, and computer simulations. Secondly, results from the main experiments will be presented. Among the main results are those on spouting characteristics, vanadium conversion, salt losses, entrainment of particles, and other items of concern such as fusing of the bed.

Note on Experimental Limitations

It was desired to perform more experiments than were made to investigate repeatability as well as to study a wider range of variables. However, the number of experiments that could be performed were limited by the supplying of particles by the Centre de Recherches Minérales. The supply of larger particles ended with a second delivery in June 1986. Only smaller particles were available for the remainder of this part of the project. However, with the given system the use of these smaller particles was limited.

1. Preliminary Results

1.1 Particle Size Analysis

The effect of particle size distribution is of major importance in fluidized and spouted bed operations as well as in solid-solid reaction kinetics. To that purpose, the particle size distribution was determined for all batches received from the Centre de Recherches Minérales as well as of samples prepared in ways that alter the particle size distribution. Determination was conducted with a vibrating sieving apparatus.

Figure 5-1 shows the particle size distribution for the original vanadium ore concentrate. This can be compared with the particle size distribution of the later vanadium ore concentrate which is coarser (Figure 5-2). Figure 5-3 gives the particle size distribution for Na_2CO_3, used most commonly. The salt constitutes up to 10% of the total sample by weight, and thus has a significant effect on the overall particle size distribution. Considerable agglomeration of the particles occurred when the salt-dissolving process was used to prepare the samples as shown in Figure 5-4. A particle size distribution of particles after a typical run is shown in Figure 5-5.

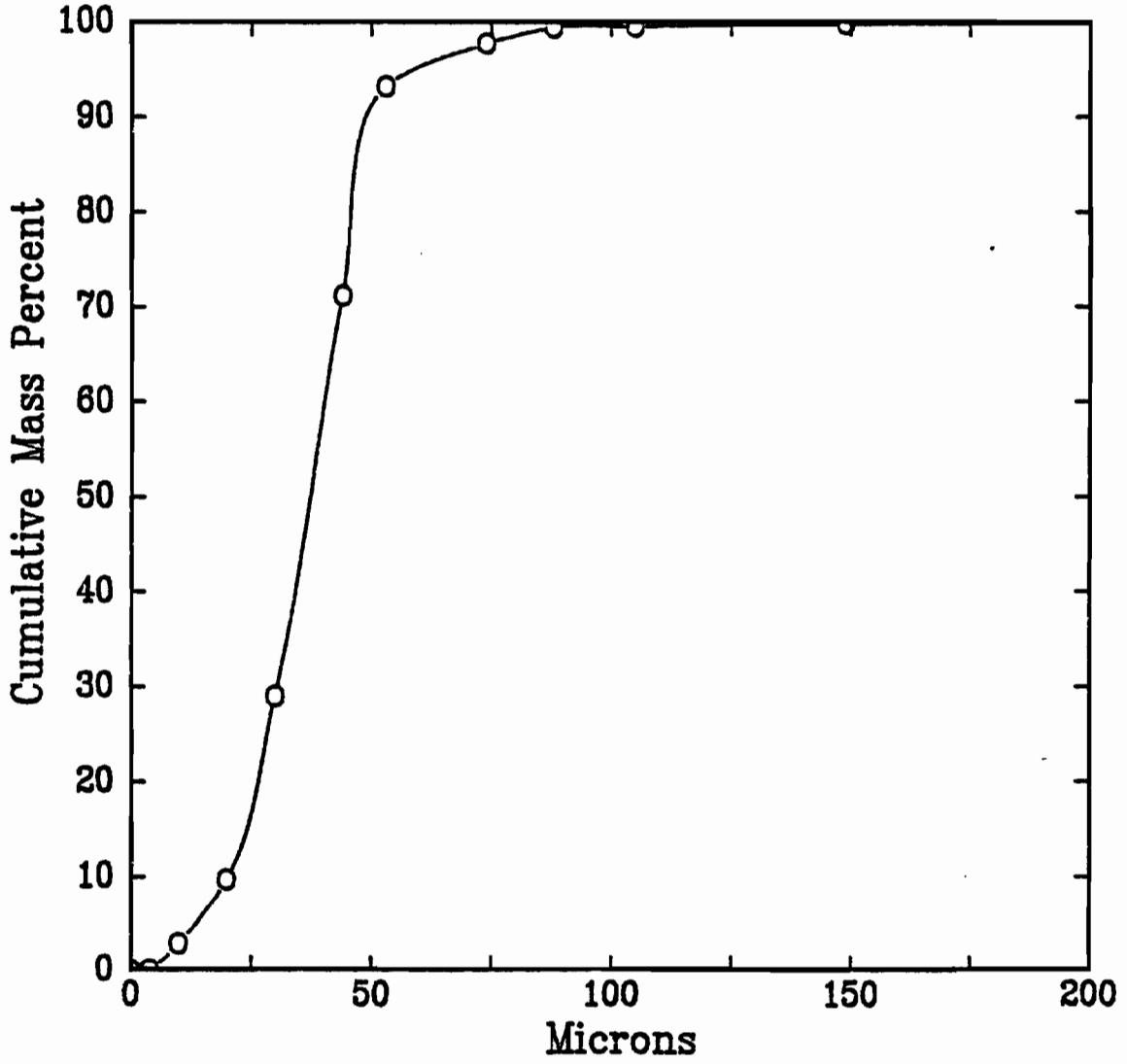

Figure 5-1 - Particle Size Distribution for Smaller Particles

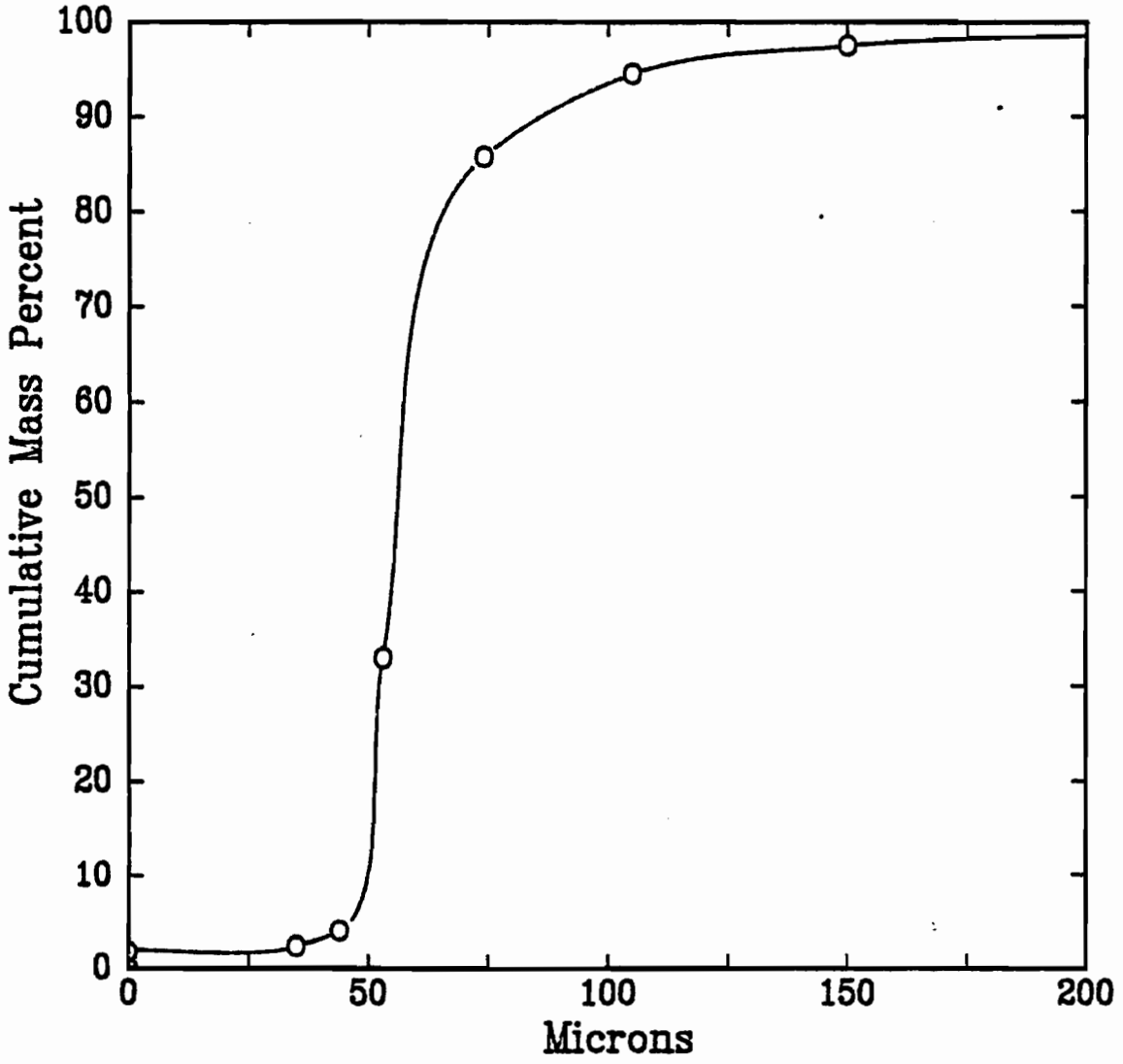

Figure 5-2 - Particle Size Distribution for Larger Particles

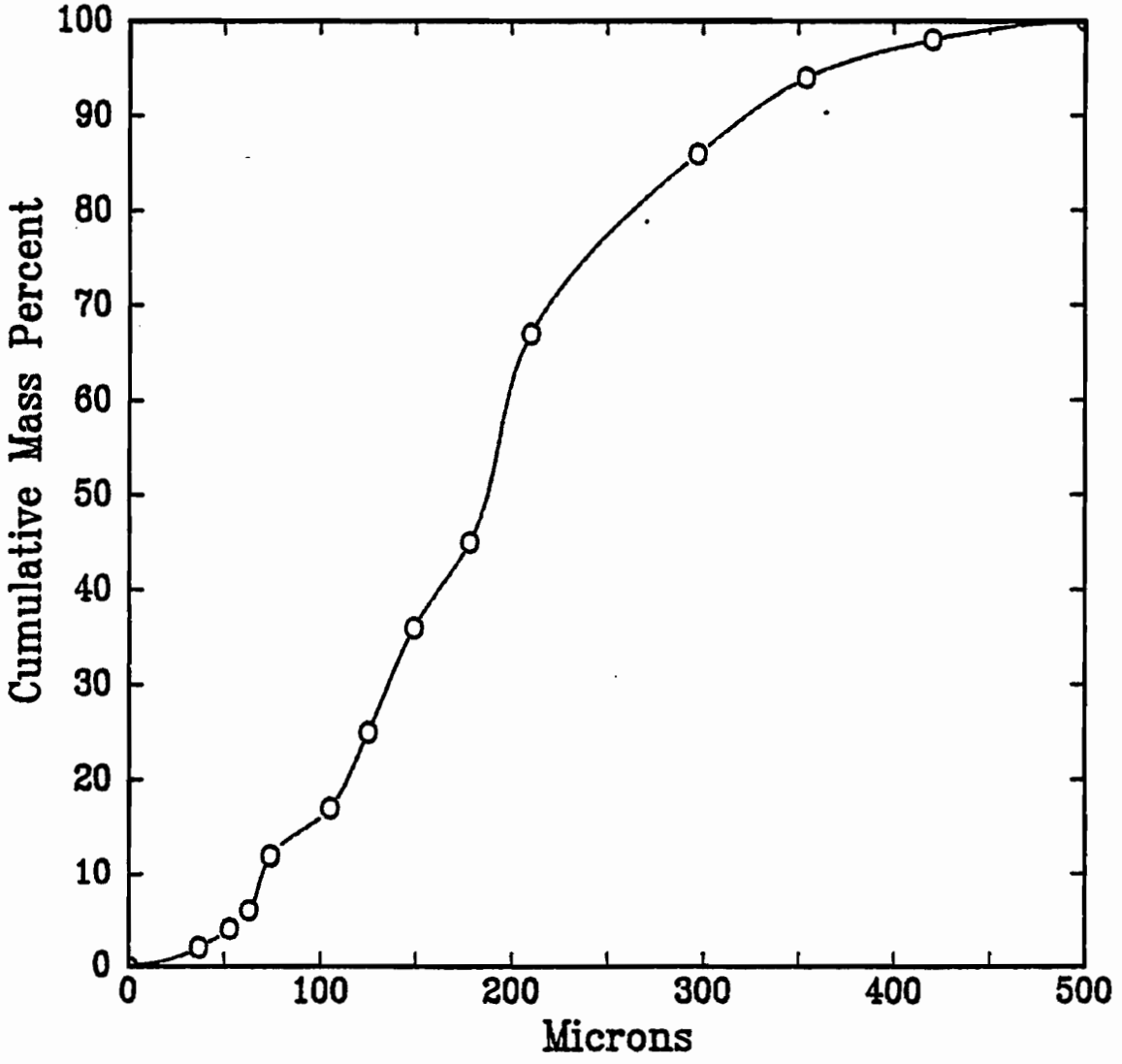

Figure 5-3 - Particle Size Distribution for Na_2CO_3

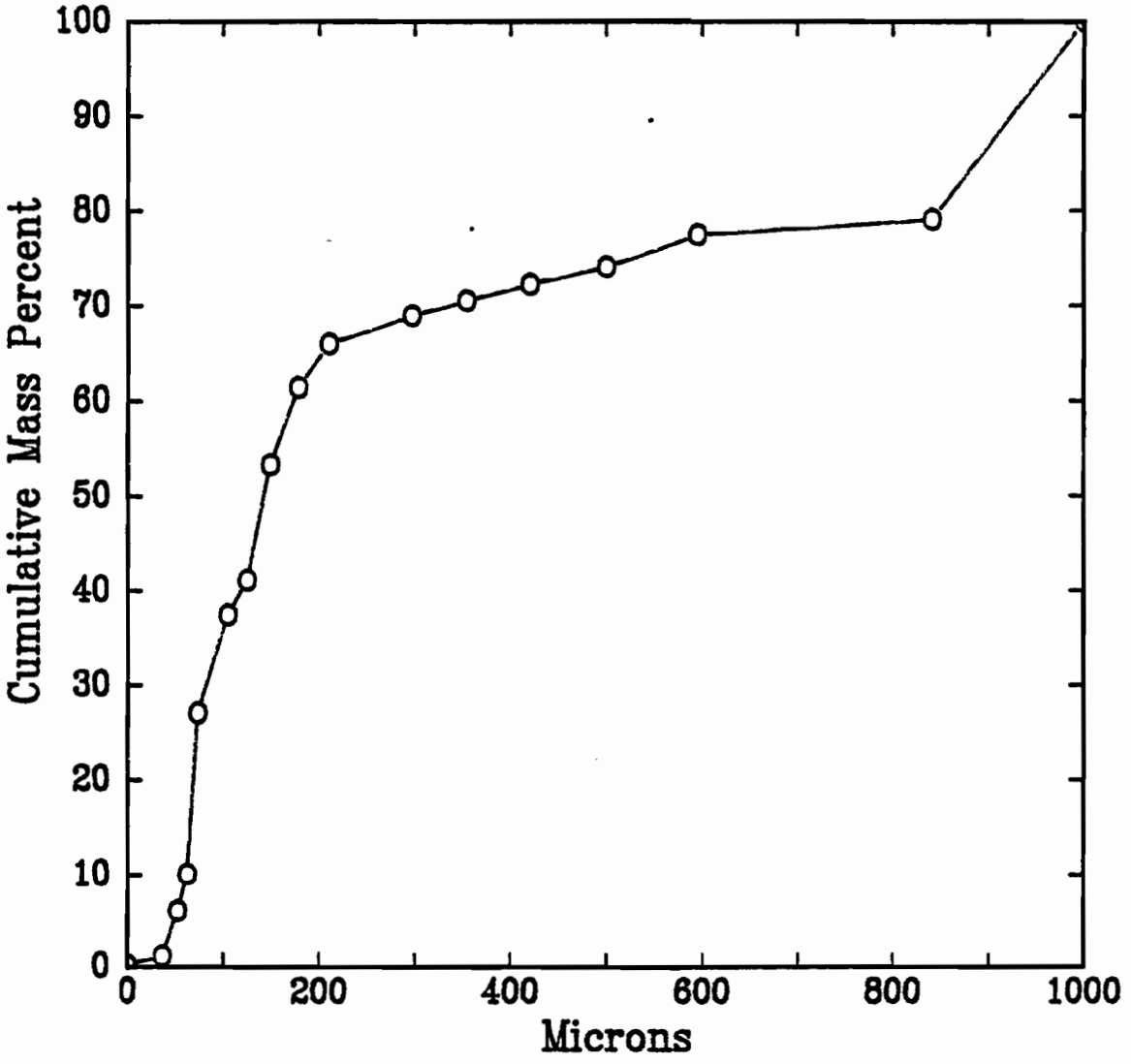

Figure 5-4 - Particle Size Distribution for Agglomerated Particles

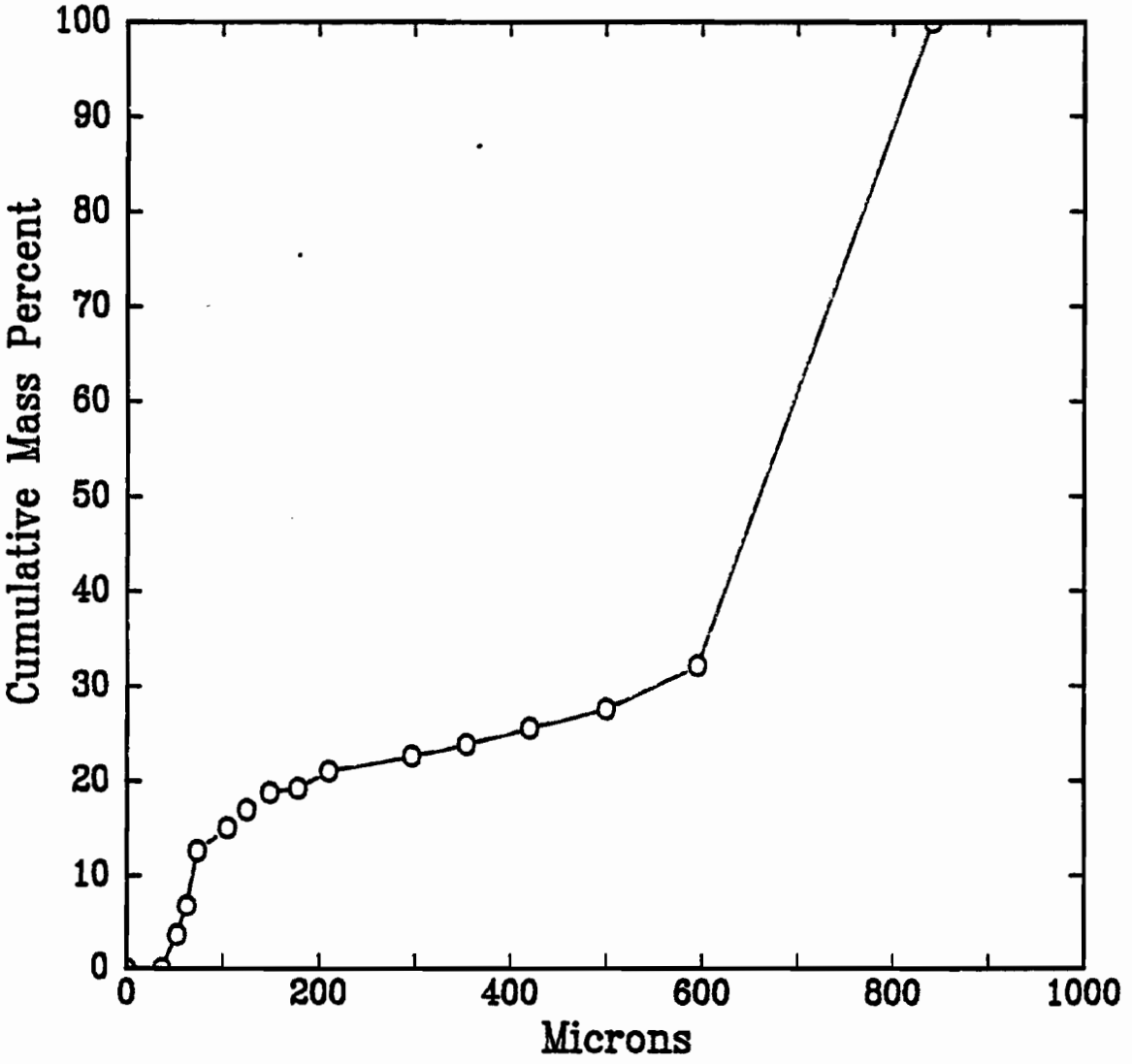

Figure 5-5 - Particle Size Distribution for Larger Particles After a Typical Run (9kW, 30 min)

1.2 Fluidization Characteristics

Though the equipment incorporates a spouted and not a fluidized bed, the determination of some fluidization characteristics of the two supplied particle size distributions was of interest. Figure 5-6 shows a typical fluidization curve obtained for the larger particles. A similar curve could not be obtained on a consistent basis for smaller particles and is thus not included. The curve was obtained from measurements in a small plexiglass fluidized bed with a 5 cm diameter.

1.3 Computer Simulations

1.3.1 Temperature Predictions

The temperatures experienced in plasma flames can be extremely high. In order to have guidelines for the temperatures to be expected in the reactor at various conditions, the F*A*C*T (Facility for the Analysis of Chemical Thermodynamics, see Appendix A) computer system running on the university mainframe was used. Figures 5-7 and 5-8 show the curves for predicted flame temperatures with variations in net power input and air injection with the torch being fired with nitrogen at 25 lpm and argon at 15 lpm. The predictions are based simply on an energy

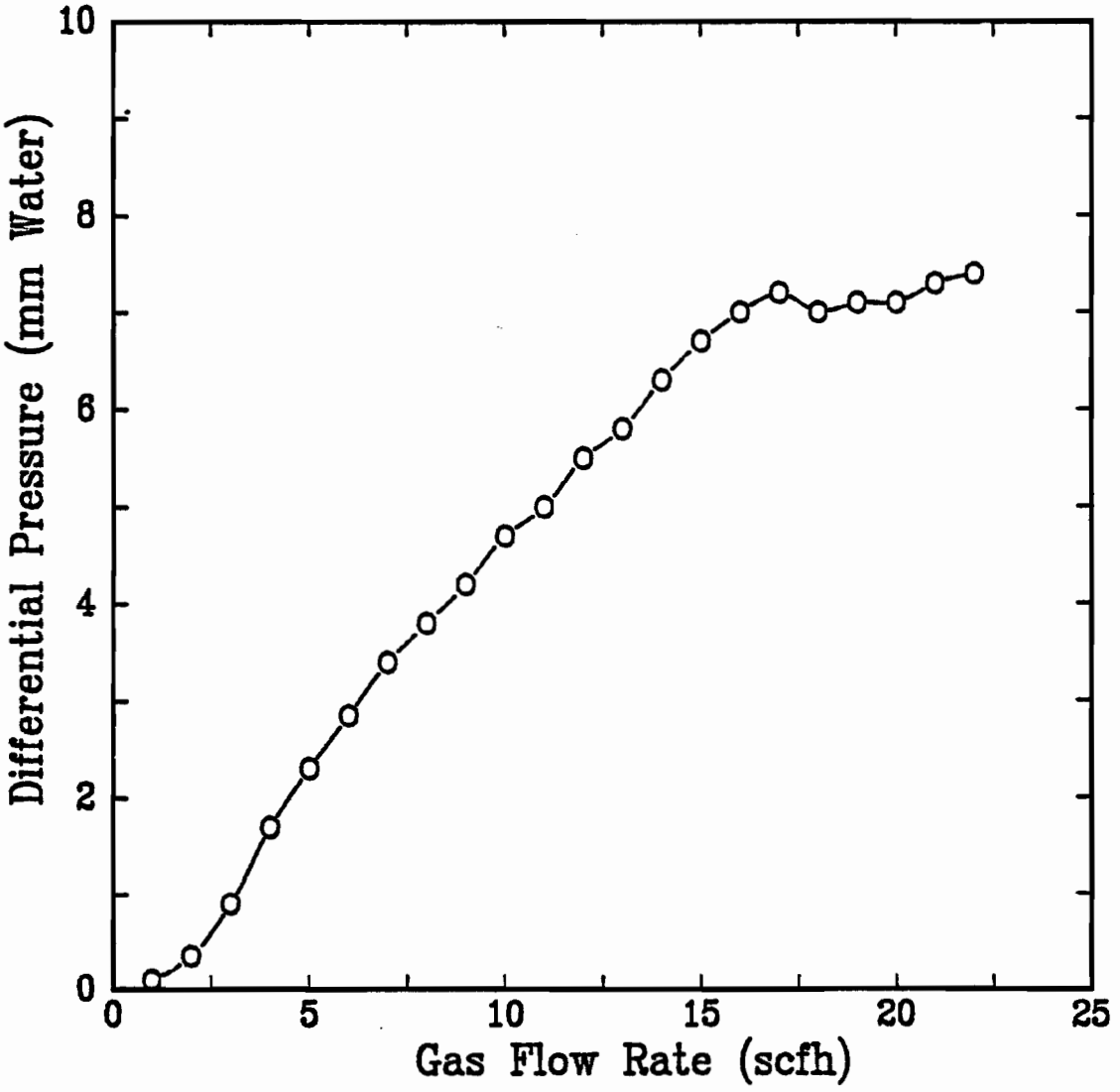

Figure 5-6 - Fluidization Curve

l/d = 1, large particles

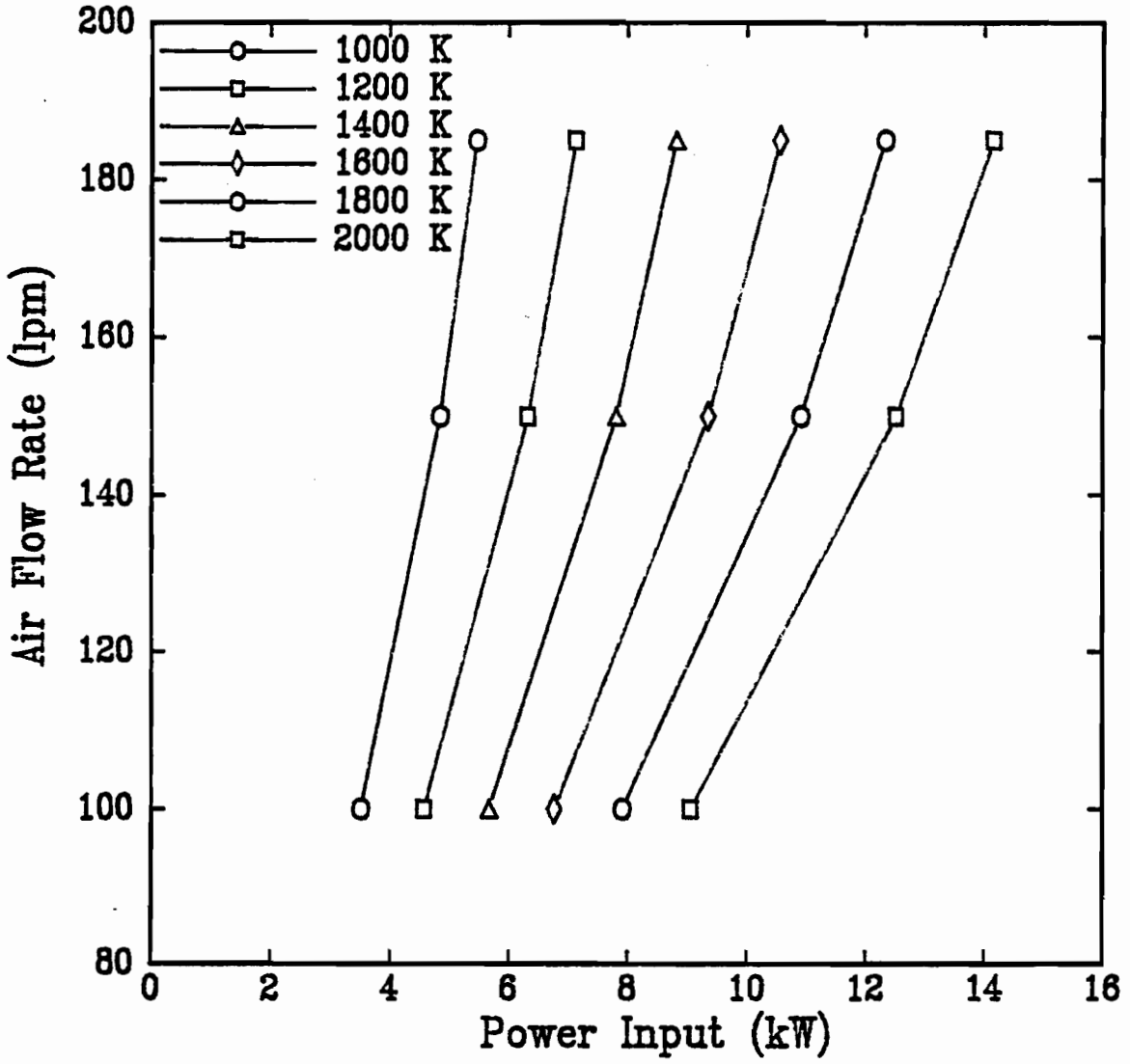

Figure 5-7 - Predicted Flame Temperature

Torch efficiency = 65 %

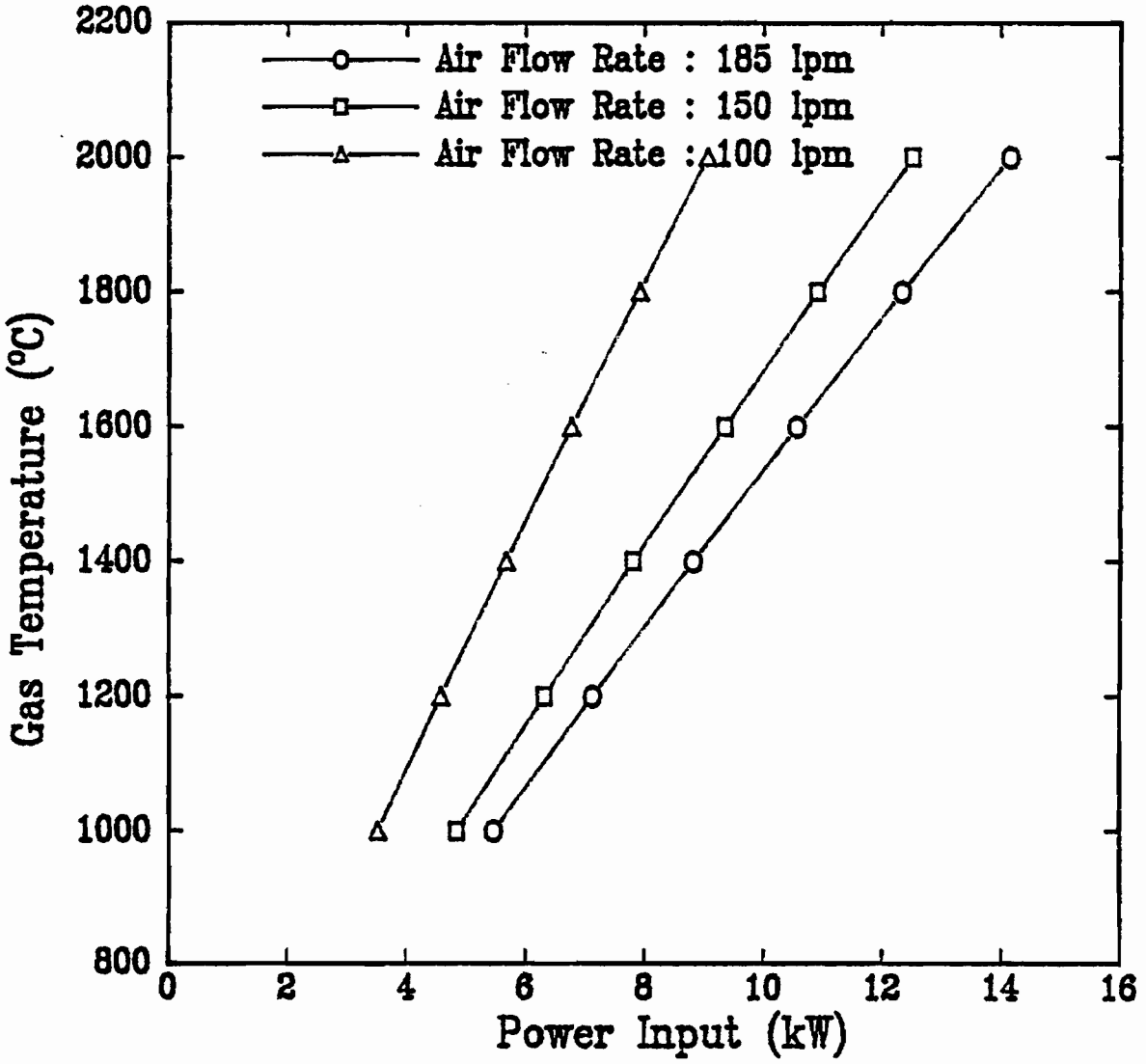

Figure 5-8 - Predicted Flame Temperature

Torch efficiency = 65 %

balance around the torch operation, at a fixed efficiency of 65%.

1.3.2 Reaction Simulations

To verify that the desired reactions were thermodynamically feasible, they were simulated on F*A*C*T. It was initially attempted to completely represent the reaction with all the constituents. This however, would suggest 6 elements (V, Fe, Ti, O, Na, Cl or S or C or H). F*A*C*T does not allow for more than 5 elements to be considered as reactant components. In addition, an extreme number of possible products results. As it turns out, the predominant reaction is the one between the V_2O_5 and the sodium salt. All other reactants react only minimally to form insignificant amounts of products. Therefore, V_2O_5 + <Salt> = <Products> is the reaction fed into F*A*C*T. This greatly reduces computation time and does not affect the principal results.

The equilibrium temperature of the products has been set equal to that of the reactants since the products will be separated (gases from solids) while at the equilibrium temperature. In addition, the pressure of both the reactants and the products has been set to 1 atm. Though the pressures may differ in the actual reactor, the principal products of interest are solid, and will thus not be greatly affected by pressure. The

printed results of several EQUILIB runs are found in Appendix B-1.

TABLE IX

Variation of Salts

Salt	Product produced	Efficiency
NaCl	0.75 moles/mole V_2O_5	75 %
NaOH	1.00 moles/mole V_2O_5	100 %
Na_2CO_3	1.00 moles/mole V_2O_5	100 %
Na_2SO_4	1.00 moles/mole V_2O_5	100 %

'Product produced' refers to the amount of sodium vanadate produced for every mole of V_2O_5 fed as reactant. Efficiency is defined by the percentage of total vanadium converted to sodium metavanadate. Runs performed at 900 K are tabulated above. A temperature range from 700 to 1200 K was studied with no change in the results.

Varying the reaction temperature in the 800 - 1200 K range was found to alter the equilibrium composition only minimally. The equilibrium composition of the sodium metavanadate was found to be unaffected by such a temperature change.

Additionally, F*A*C*T was run to determine whether the ilmenite and magnetite in the concentrate would consume any sodium carbonate at the given conditions. A sample printout of

an EQUILIB run is given in Appendix B-2. It was found that sodium carbonate does not react with either ilmenite or magnetite to any significant degree.

1.4 Mass Balances

A mass balance was done to calculate how much salt was theoretically necessary to convert the vanadium to sodium metavanadate.

Basis: 1000 g mineral concentrate (15 g V_2O_5)

TABLE X

Theoretical Salt Requirements

Salt	M.W.					Amount Required
NaOH	40	->	$\frac{15\ g}{182\ g/mole}$	x $\frac{2\ NaOH}{Na_2O}$	x 40 g/mole	= 6.6 g
Na_2SO_4	142	->	$\frac{15\ g}{182\ g/mole}$	x $\frac{1\ Na_2SO_4}{Na_2O}$	x 142 g/mole	= 11.7 g
Na_2CO_3	106	->	$\frac{15\ g}{182\ g/mole}$	x $\frac{1\ Na_2CO_3}{Na_2O}$	x 106 g/mole	= 8.7 g
NaCl	58.5	->	$\frac{15\ g}{182\ g/mole}$	x $\frac{2\ NaCl}{Na_2O}$	x 58.5 g/mole	= 9.6 g

1.5 Heat Balances

Calculations using the two most likely-to-be-used salts, NaCl and $NaCO_3$ were performed. 100% Na_2O to form $Na_2O-V_2O_5$ is assumed. 1000 g of ore is taken as a basis (15 g V_2O_5).

TABLE XI

Heat Balance

Energy to heat mineral, salt and gas from 298 K to 1000 K:

1200	g Fe_3O_4	767 kJ
300	g $FeO-TiO_2$	168 kJ
150	g Na_2CO_3	151 kJ
150 l	Argon (10 min run)	147 kJ
250 l	Nitrogen	244 kJ
2000 l	Air	1844 kJ
Total	=	3326 kJ

Including a 15% heat loss (assumed):

Total = 3826 kJ

Exothermic Reactions:

$2Fe_3O_4 + 1/2O_2 = 3Fe_2O_3$
$H_{1000\ K} = -643$ kJ/1200 g Fe_3O_4

$2FeO-TiO_2 + 1/2O_2 = Fe_2O_3 + 2TiO_2$
$H_{1000\ K} = -445$ kJ/300 g $FeO-TiO_2$

$Na_2CO_3 + V_2O_3 + 1/2O_2 = 2NaVO_3 + CO_2$
$H_{1000\ K} = -220$ kJ/150 g Na_2CO_3

Total Energy = 2506 kJ

1.6 Melting Point Analysis

The ore is a mixture of a variety of minerals combined in a complex matrix. It is thus not easy to estimate a melting temperature by theoretical means. At the same time, ovens available could only attain temperatures of 1000°C, which did not melt the ore. The ore was thus melted in a transferred-arc plasma furnace used for research in the McGill University Plasma Group. The melting point of the ore was determined to fall in the 1350 - 1400°C range.

From F*A*C*T the melting point of Na_2CO_3 was given as 850°C. Data on Na_2CO_3 extended to 1727°C. Na_2CO_3 is not predicted to vaporize below this temperature.

2. Main Results

2.1 Spouting Characteristics

In order to gain an increased understanding of the physical characteristics of the spouted bed in operation, photographs were taken. Figure 5-9 shows the spouting bed (without the torch being fired) at a total gas flow rate of 200 lpm.

2.2 Vanadium Conversion

The efficient conversion of the vanadium pentoxide in the ore to soluble sodium metavanadate is the one major objective of this research. It follows that the conversion was measured for all runs.

The two primary variables studied were the maximum measured bed temperature (as a function of power), and the run duration. The maximum measured bed temperature ranged from 215°C to approx. 700°C. The other conditions were kept as constant as possible, but some fluctuations were inevitable.

Figure 5-10 shows the effect of maximum measured bed temperature (as a function of input power) at different run

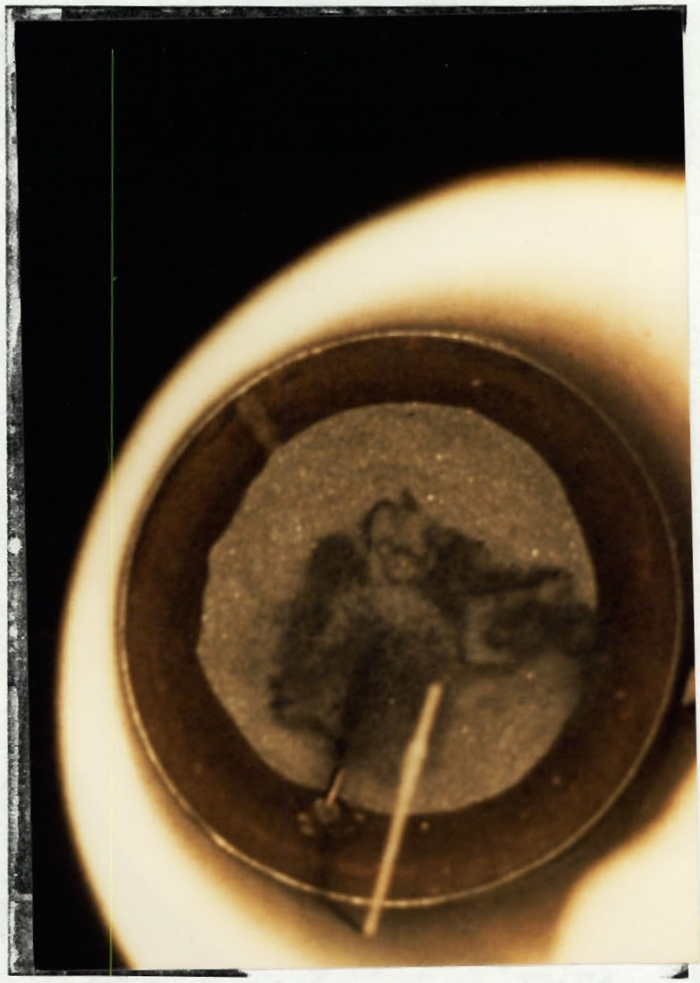

Figure 5-9 - Photograph of Spouting Bed

Total Gas Flow Rate = 200 lpm

durations on the conversion of the vanadium trioxide to sodium metavanadate. For a typical run the gas flow rates were constant at 200 lpm air, 25 lpm N_2 and 15 lpm Ar.

Finally, a third variable investigated was the particle size distribution. Four possibilities, including small and large particles as well as small agglomerated and large agglomerated particles were considered. Table XII shows the effect of using the larger or smaller particle sizes in two typical runs on the conversion of the vanadium pentoxide to sodium metavanadate with other conditions constant. The final measured bed temperature was 660°C - 670°C.

TABLE XII

Effect of Particle Size on Vanadium Conversion

9 kW, 30 min. run

Particle Size	Conversion
small agglomerated	60 %
large agglomerated	36 %

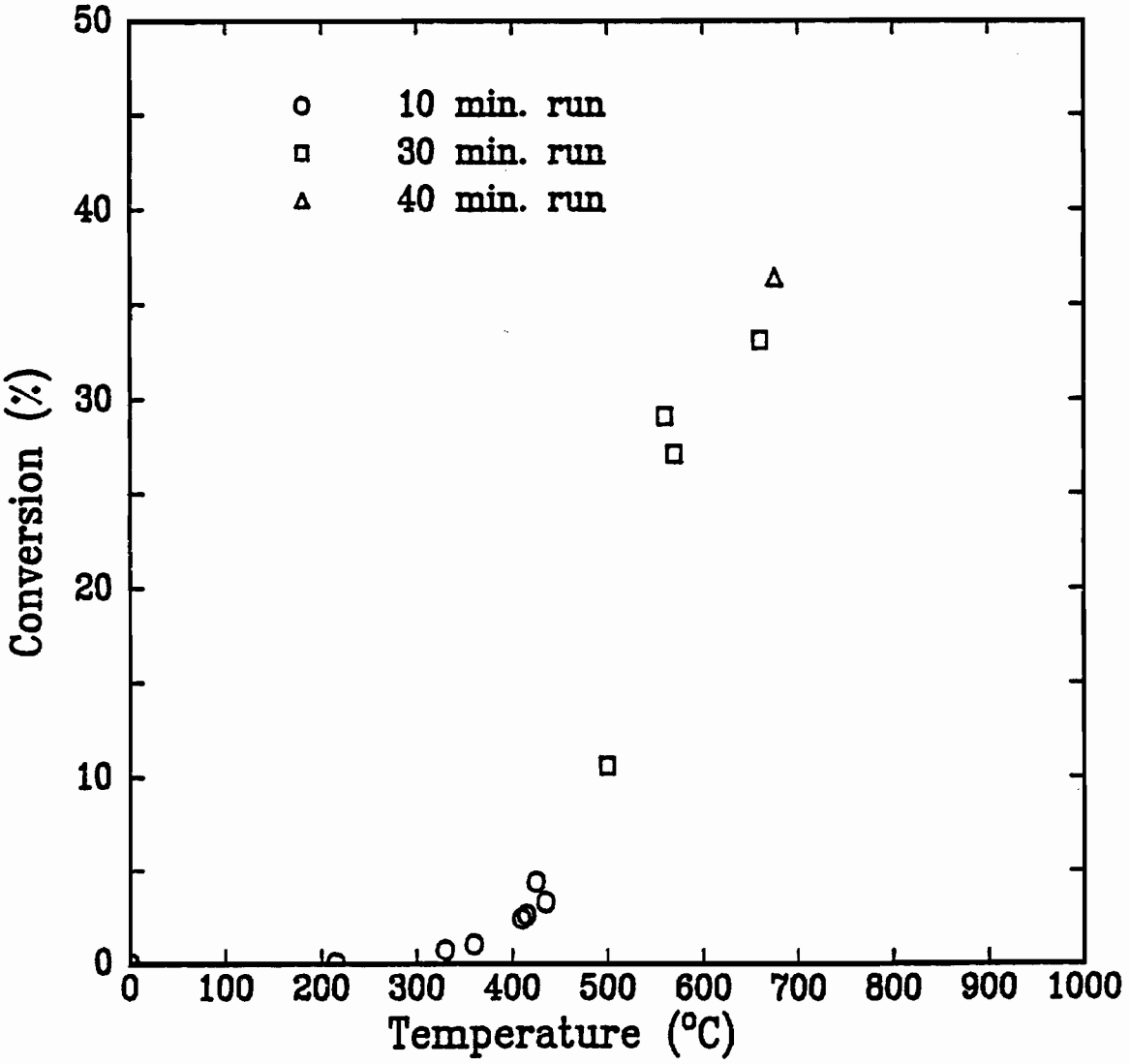

Figure 5-10 - Conversion vs. Temperature

2.3 Salt Losses

In this process, especially when using salts other than NaCl, the salt costs are a major component of the overall cost. It is thus important that the salt mixed with the ore is consumed as efficiently as possible and that entrainment of vaporized salt into the effluent is minimized.

Figure 5-11 shows the contents of sodium salt in the remaining bed after a typical run, divided into the three constituents. Figure 5-12 gives the distribution on an absolute basis by weight taking into account the different amounts of the the three constituents. A typical run was at 9 kW, with a duration of 30 minutes. Gas flow rates were constant at 25 lpm nitrogen and 15 lpm argon to the torch, and 200 lpm air to the manifold.

Figure 5-13 compares the distribution by absolute weight between the remainder of the bed (all three constituents together) with the contents of the bag filter using larger agglomerated particles. A third column shows the amount that could not be accounted for. The unaccounted salt losses can be attributed to small condensed salt particles not being caught by the filter, as well as salt condensation inside the reactor. By visual inspection however, condensation inside the reactor was

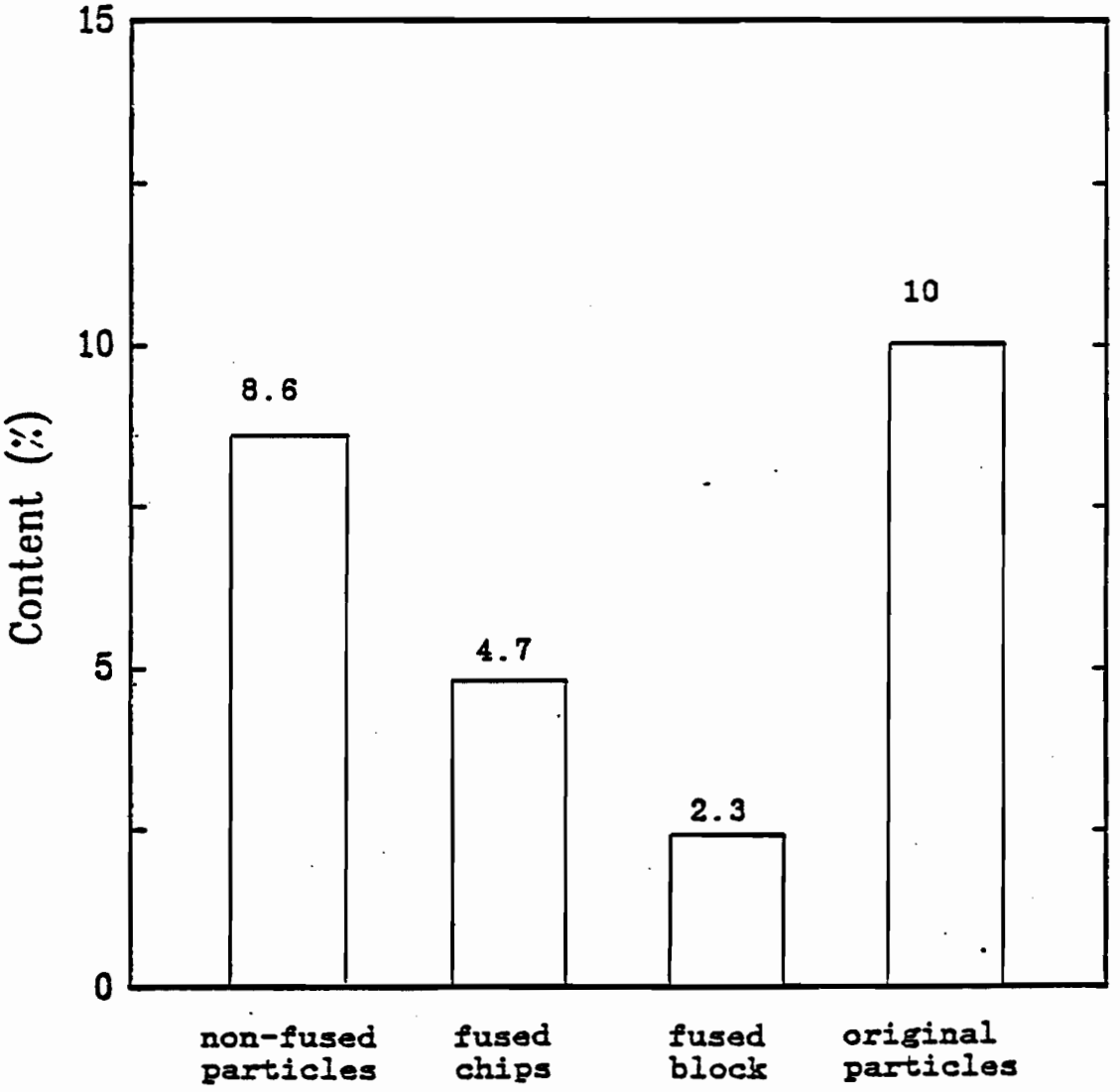

Figure 5-11 - Sodium Salt Distribution in Bed after Run 9 kW, 30 min.

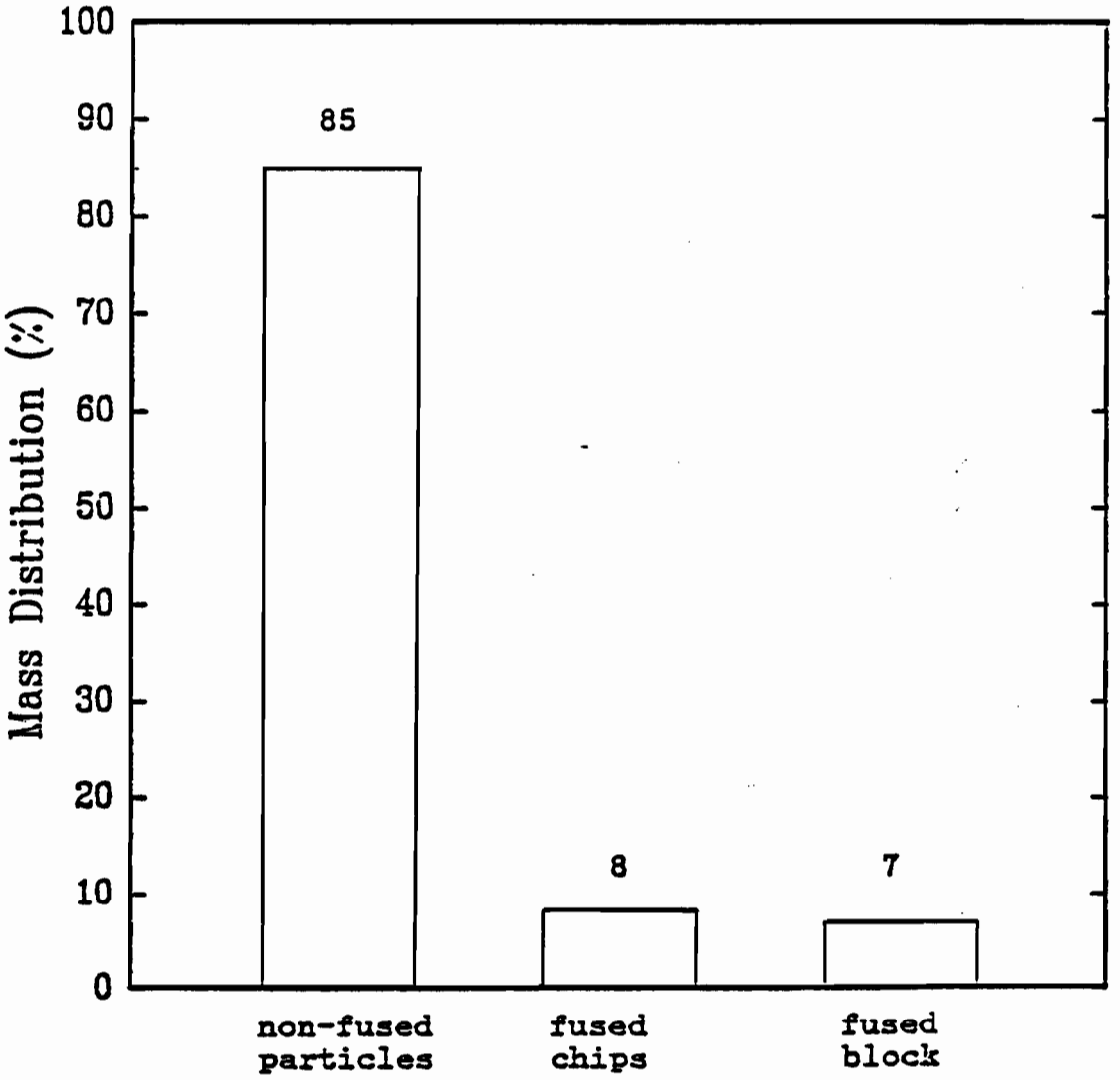

Figure 5-12 - Sodium Salt Distribution in Bed after Run 9 kW, 30 min.

insignificant. Also, with F*A*C*T no undesirable parallel reactions using sodium carbonate are predicted. Figure 5-14 makes the same comparison when using smaller agglomerated particles.

Finally, Table XIII compares the sodium salt content of the bag filter contents after a typical run using smaller and larger agglomerated particles.

TABLE XIII

Effect of Particle Size on Bag Filter Salt Content

9 kW, 30 min. run

Particle Size	Salt to Concentrate Ratio	Entrainment %
Original particles	1	-
small agglomerated	0.75	30
large agglomerated	1.4	7

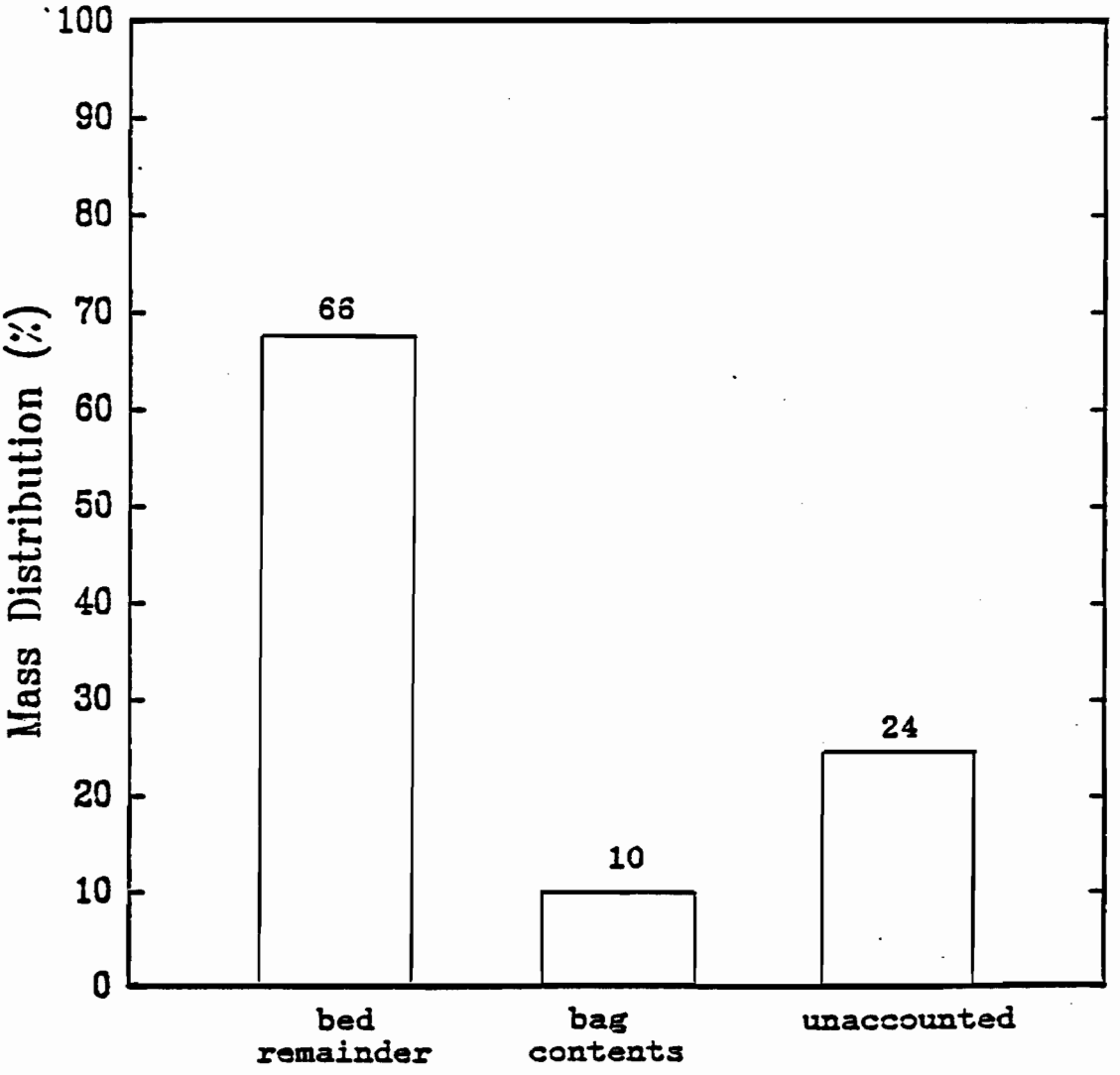

Figure 5-13 - Sodium Salt Distribution after Run Larger Particles, 9 kW, 30 min.

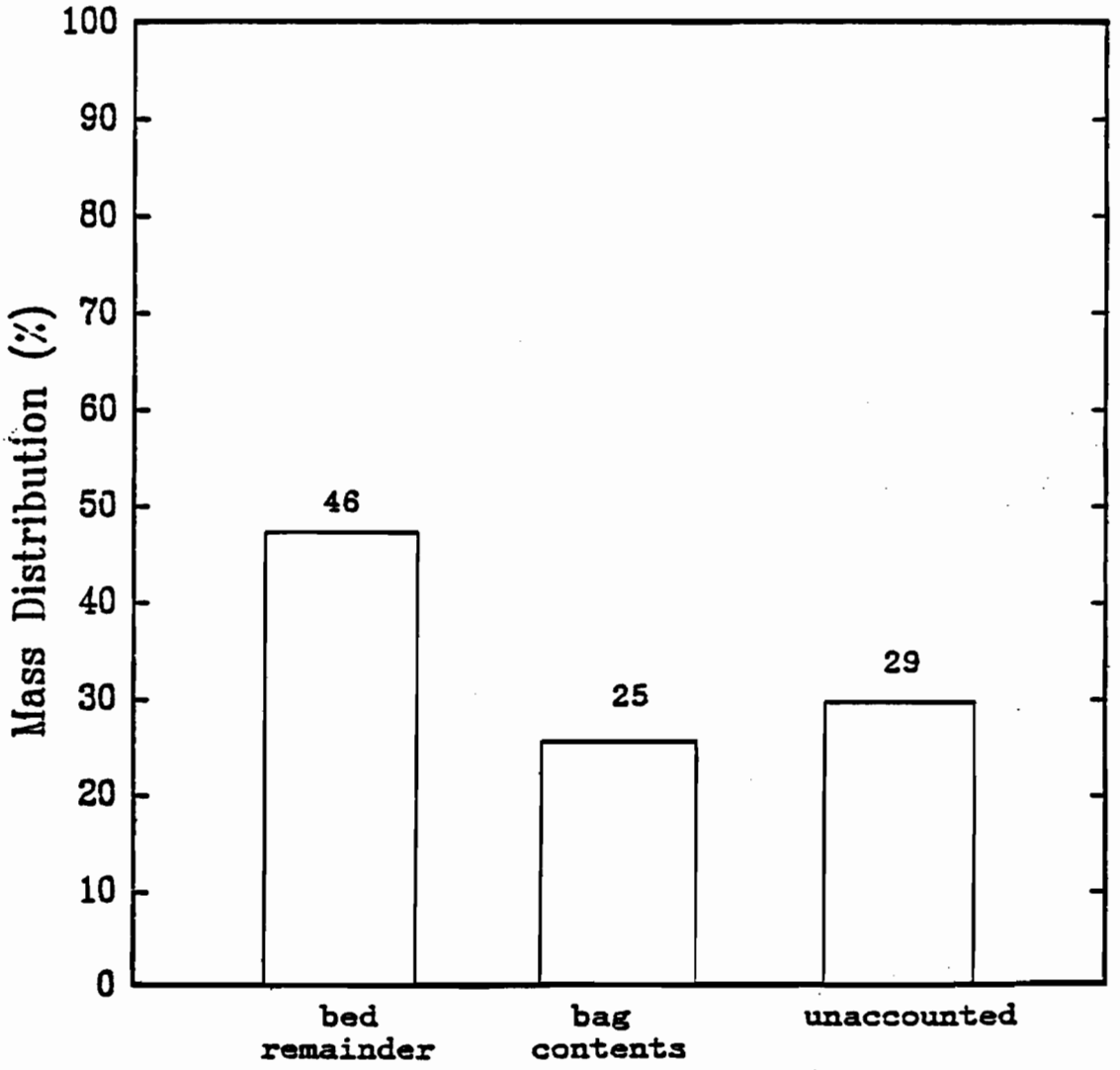

Figure 5-14 - Sodium Salt Distribution after Run Smaller Particles, 9 kW, 30 min.

2.4 Entrainment

Excessive entrainment of finer ore particles into the effluent must be minimized. Not only does the entrainment represent lost potential vanadium, but also the possibility of equipment complications such as clogging of pipes. Though auxiliary equipment can be installed to catch and recirculate the material into the reactor, this involves increased equipment cost and complexity.

Figure 5-15 shows the effect of run duration at constant power on the amount of concentrate entrained.

Table XIV shows the effect of particle size distribution the amount of concentrate entrained with other conditions constant (power of 9 kW, duration of 30 minutes, nitrogen at 25 lpm, argon at 15 lpm and air at 200 lpm).

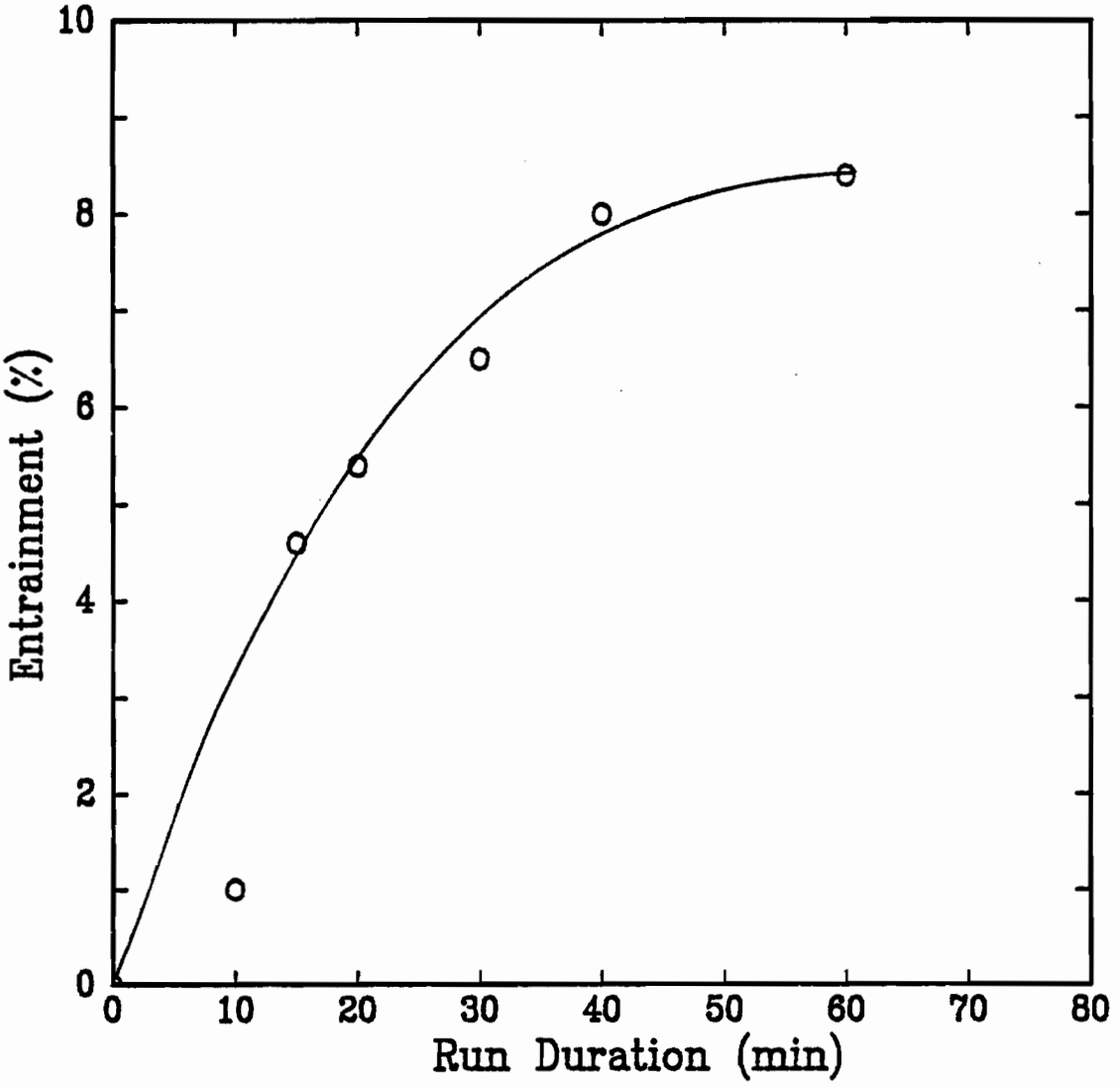

Figure 5-15 - Particle Entrainment vs. Run Duration

Larger Particles

TABLE XIV

Effect of Particle Size on Entrainment

9 kW, 30 min. run

Particle Size	Entrainment
small agglomerated	30 %
large agglomerated	8.0 %

2.5 Bed Fusing

One of the most difficult problems encountered was the fusing of the bed at certain conditions. The definition of fusing is a portion of the particles fusing together to make one or few solid blocks, impeding any additional circulation in the bed of the remaining particles. This condition could be observed when the plasma flame shot through the central hole of the block uninterruptedly (See Figure 5-16).

Figure 5-17 shows the effect of input power on the percentage of particles fusing at run durations of 30 minutes.

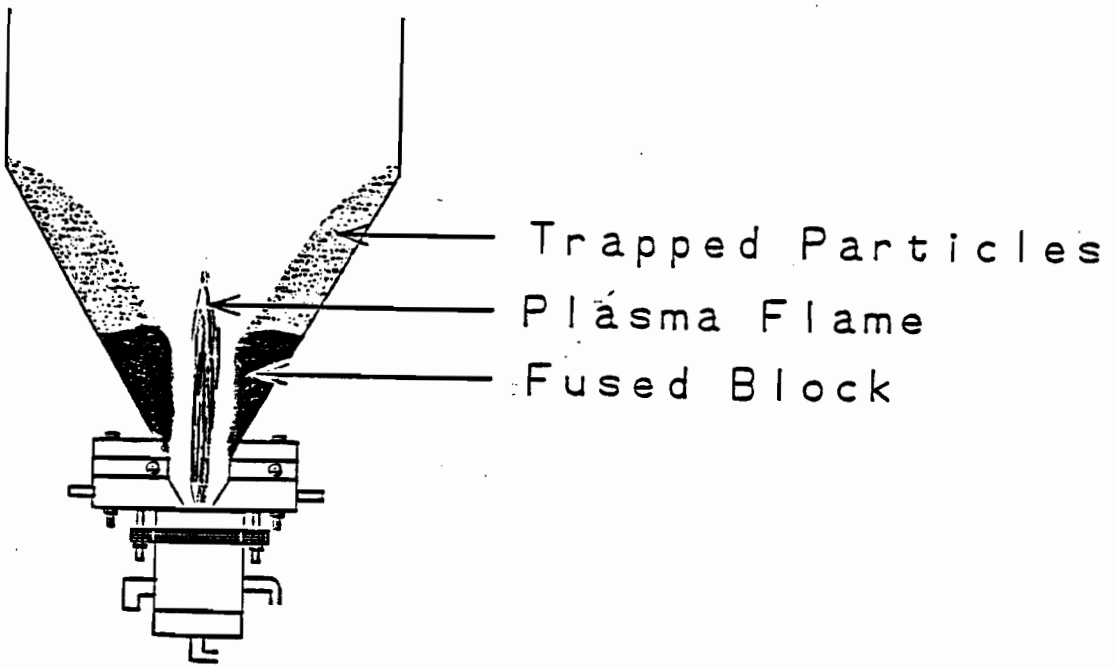

Figure 5-16 - Schematic of a Fused Bed

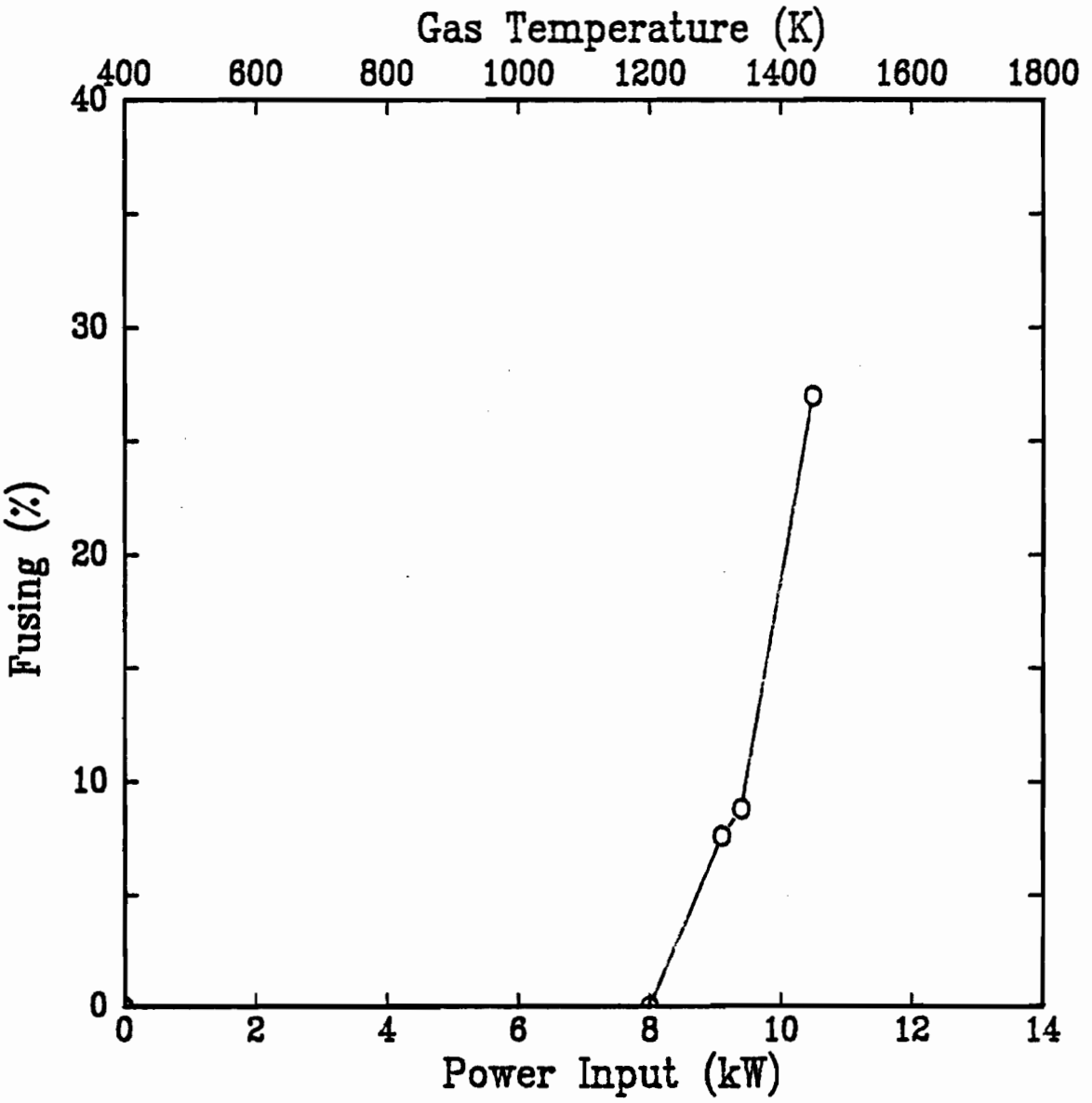

Figure 5-17 - Particle Fusing vs. Input Power

Larger Particles, 30 min.

Figure 5-18 shows the effect of run duration at constant power on the percentage of particles fusing.

Table XV shows the effect of particle size distribution on the percentage of particles fusing, with other conditions constant (power of 9 kW, duration of 30 minutes, nitrogen at 25 lpm, argon at 15 lpm and air at 200 lpm).

TABLE XV

Effect of Particle Size on the Degree of Bed Fusing

9 kW, 30 min. run

Particle Size	Fusing
small agglomerated	33 %
large agglomerated	8.8 %

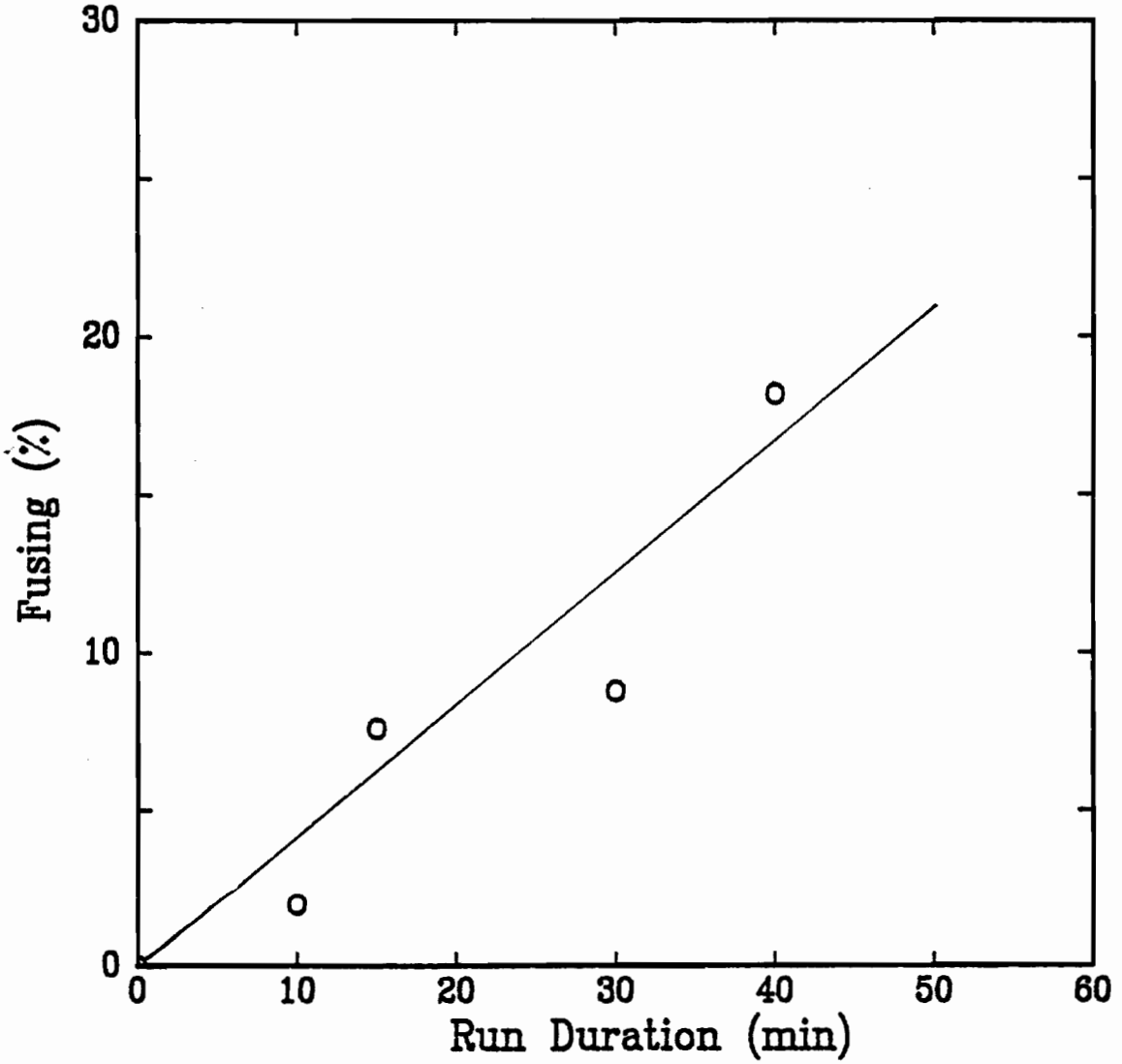

Figure 5-18 - Particle Fusing vs. Run Duration

Larger Particles, 9 kW

CHAPTER VI

DISCUSSION

1. Preliminary

1.1 Equipment Construction

About six months were spent on commissioning experiments as well as main experiments. Commissioning experiments included testing of the torch, the water cooling arrangement, and other equipment.

A problem with the plasma torch was encountered early in the project. Due to reasons not quite clear, the arc frequently moved out of the actual torch and shot to the inside cone of the bottom flange. This would result in a perforation of the cone wall, ensuing a water leak into the reactor. Various parameters such as gas flow rates, different cathode shapes etc. were changed in an attempt to solve this problem. After these alternatives failed to provide a satisfactory solution, the inside cone was fitted with a boron nitrite cover which eliminated the problem. Beyond this obstacle, the torch proved itself as a reliable unit throughout the project. Common plasma torch operation difficulties such as internal water leaks, excessive electrode erosion, over-heating or arc extinguishing were not encountered. A plasma torch lends itself to process automation and continuous control, and this was confirmed in this project.

1.2 Fluidization

The literature often points out that as the particle size decreases below a certain level, it becomes increasingly difficult to attain satisfactory fluidization. This was confirmed by the preliminary experiments on fluidization. From the particle size analyses, it was ascertained that the provided samples were exceedingly small for fluidization purposes. Whereas the larger particles could be fluidized quite adequately, the smaller could not on a consistent basis. Channelling became predominant, and at times the whole bed would travel up the plexiglas vessel in a slug.

The conclusion follows that the finer particles are harder to fluidize, and one may infer that fluidization is altogether impossible. However, different conditions, particularly in vessel size, may prove such a conclusion premature. The model fluidized bed had a diameter of 5 cm. This can result in a substantial effect of the walls, especially when operating under dry air conditions where some particles were noticed to stick to the wall. In addition, the experiments were done with vessel length/diameter > 1. With small particles, this can easily lead to slugging. Preliminary experiments with larger vessels are planned.

1.3 Computer Simulations

The direct measurement of the plasma flame temperature is quite difficult and not really necessary for this project. Nevertheless, an approximation of this temperature was desired. The simulations through F*A*C*T show that a variation of power and air flow rate can give temperatures within a wide range. Generally, a gas temperature allowing the bed to heat up rapidly heat-up without melting the particles was desired. The plasma flame was always mixed with a stream of air giving a temperature of around 1300 K at typical experimental conditions. This is below the determined particle melting temperature.

From thermodynamics it is predicted that full conversion is attained within the investigated 800 - 1200°C range. The conversions for all salts except NaCl were predicted to be 100%. Of course, computer simulations can only be taken as a starting point, as too many factors are not taken into account. In addition, F*A*C*T only calculates equilibrium conditions, without any kinetic considerations. The presence of interfering compounds, physical limitations (e.g. poor contacting), fluctuations in conditions, are among a few other factors that can preclude the predicted outcome.

1.4 Heat Balance Calculations

Taking into account as many of the aspects involved, a basic heat balance was established. The energy requirement for a typical loading of particles was calculated as 2506 kJ for a 10-minute run. At the same time, the torch is typically running at 9 kW. With an estimated efficiency of 65% the torch supplies 3510 kJ to the reactor. It can be concluded that barring excessive heat losses (by conduction to reactor walls, to effluent gas etc.), the power requirements are fulfilled.

2. Main Experiments

2.1 Overall Viability

The second major objective of the project is demonstrating that the desired reaction could be achieved with the equipment. A general discussion of the qualitative aspects of the experiments follows. From the presented results it can be seen quite clearly that although the process needs to be optimized, the reaction can be realized with the equipment.

2.2 Spouting

The literature states quite clearly that spouting is impossible with particles of the given sizes. At the same time, the conditions found in a plasma spouted bed are different than in conventional spouted beds. Primarily, due to the very high velocities involved, the momentum of the gas is much higher than in conventional spouted beds.

Proper spouting was impossible on a consistent basis with the smaller particles. With the larger particles (though still very small for spouted beds), the spouting attained is not true spouting but what may loosely be called 'bubble spouting'. With

bubble-spouting, the particles do not follow the overall circulation pattern in a steady, continuous fashion. Instead, the bed erupts in a consistent series of bursts, throwing particles from the central spout onto the top of the surrounding annulus. This was observed during experiments, and can also be seen from the photographs (Figure 5-9). The overall flow direction is similar to that of a truly spouting bed, but the particles may stay in any one location for longer durations. The degree of circulation may be satisfactory but is less than with a truly spouting bed. This proved to be one of the most critical aspects of suitable operation of the bed.

The degree of circulation was usually not as good as desired. Especially with the use of the smaller particles resulting in insufficient circulation, fusing became a serious problem. Though with the optimization of the gas flow rates and the addition of a pneumatic vibrator, circulation was improved (confirmed by decreased fusing), it was inadequate for continuous operation. However, since for future experiments the smaller particles have to be used, a major design change will be implemented in the second stage of the project (See Conclusions & Recommendations).

Nevertheless, the investigations into the spouting characteristics of the given set-up provided valuable information. In

particular, the purpose of the spouting experiments was achieved in that they direct the way to a design change that has a high probability of success.

2.3 Vanadium Conversion

The raison d'être of this project is the extraction of vanadium from Lac Doré vanadium ore. It has been shown that a plasma spouted bed can indeed be used to accomplish the desired process. However, the fact that it can be done does not imply that it is worthwhile to do so on an industrial scale. The efficiency of the process must be looked at in detail.

The present design is by no means the final one. Several changes that will improve the conversions obtained are planned and already in the design stage. Nevertheless, the results obtained were quite promising and do provide information on the reaction characteristics.

When evaluating the results obtained for a constant run duration of 10 or 30 minutes, it is clear that the temperature has a significant effect on the conversion. At a constant run duration of 30 minutes, an increase of measured bed temperature

from 500°C to 660°C results in a three-fold increase of conversion from 11% to 33%.

The literature discloses that maximum conversion of around 90 % is obtained in the 800-850°C range.(13) Extrapolating from the given data that goes to 700°C, it can be seen that the behavior seems to follow this claim. With the improved design allowing for higher temperatures, higher conversions should also be attainable.

For all experiments it was found that the fused particles had higher conversions of vanadium than the unfused particles. This could vary by a factor of 3. It can be assumed quite reasonably that the fused particles experienced higher temperatures than the unfused particles. Thus it is expected that the fused particles exhibit higher degrees of vanadium conversion than the unfused particles.

It is not surprising that when the smaller particles are used, the conversion of the vanadium also improves. In fact, the effect of using the smaller particle size over the larger size (other conditions constant) was quite marked, resulting in a increase from 36 % to 60 %. This may be attributed to the fact that a decrease in particle size resulting in rapidly increasing

particle-air as well as particle-salt contact ratio, which in turn increases the extent of the reaction.

2.5 Salt Losses

The main causes for losses of sodium salt are directly by entrainment with the particles and by vaporization. Losses by direct entrainment is a lesser cause for concern as this salt can be recirculated into the bed along with the particles by using a cyclone (see 2.6). Loss by vaporization is a more significant problem as the vaporized salt may subsequently condense anywhere along the exhaust route, and even within the reactor. In addition it may not recrystallize into a size large enough to be caught by a cyclone or bag filter.

When examining Figure 5-11, one finds that the fused particles in the bed have a significantly lower salt concentration than the non-fused particles. It can be supposed that the fused particles experienced higher temperatures. No reactions between sodium carbonate with ilmenite or magnetite are predicted. Thus, one can deduce that sodium salt is lost by vaporization.

A comparison of Figures 5-13 and 5-14 shows that the loss of sodium salt is significantly higher when using smaller particles.

Whereas 66 % by weight of the original salt (taking into account the small amount used in reaction) stayed in the bed in its original form, only 46 % stayed in the finer particles. With smaller particles, excessive fusing causes certain parts of the bed to be exposed to high temperatures. Thus more salt could evaporate.

A certain amount (24 % for larger particles, 29 % for smaller particles) could not be accounted for. This amount was either consumed by undesirable parallel reactions, condensed along the effluent route, or was not caught by the bag filter.

2.6 Entrainment

For economic reasons, it is desired to keep the entrainment of particles out of the reactor to a minimum. As the particles are very small and the gas flow rates quite high, the possibility of high entrainment does exist.

To prevent excessive entrainment, the reactor was fitted with an internal deflector plate. However, a fair amount of entrainment was still encountered. At 10 minute run durations, entrainment was around 1 %. It must be added though that at the lower duration lengths, the bed temperature was also significantly lower. With increased run durations, the rate of entrain-

ment quickly rose. After 40 minutes, entrainment leveled off at approximately 8 %. Since entrainment levels off with time, it can be deduced that attrition of the particles is not significant.

Not surprisingly, use of the smaller particles significantly increases the degree of entrainment. Using the larger particles, the maximum rate of entrainment encountered was 8 %. At the same conditions, the smaller particles resulted in an entrainment close to 30 %.

These results could be expected. As the run duration is increased, the rate of entrainment rises initially as particles at the lower end of the particle size distribution spectrum are entrained. Eventually though, all of the finer particles are entrained and the larger particles remaining are too heavy to be entrained. In addition, increased agglomeration of the particles also reduces the likelihood of entrainment.

For larger particles, the rate of entrainment is not excessive but can be substantial when considering economic as well as enviromental concerns. Nevertheless, the problem could probably easily be solved by the addition of a cyclone to the system. The particles collected in the cyclone can then be recirculated into the bed. With a net increase in particle size due to agglomera-

tion, a steady state should eventually be attainable. This may be especially easy to institute in a continuous operation system. In addition, a change in the reactor shell design (e.g. larger discharge zone) could also decrease entrainment.

2.7 Fusing

Clearly the main problem encountered was that of fusing. Even though the mean bed temperatures were always below the ore melting temperature, sintering regularly caused partial fusing of the bed. At certain conditions the degree of fusing became completely unacceptable. The degree of fusing is considered unacceptable when it prevents the remaining unfused particles from circulating properly. The degree of fusing is a function of temperature as well as run duration.

It may make more sense to compare the degree of fusing directly to the mean bed temperature. However this falsely represents the situation. Most of the particles do not sinter when they are in the bed, but as they pass through the hot flame. Thus in a situation where the bed is heated rapidly with a very hot flame but the bed itself is still relatively cold, the degree of fusing may be higher than in a gently heated bed which is hotter. It thus makes more sense to compare the flame temperature to the degree of fusing directly. The temperature of the

flame is a function of the gas flow rates and the torch power input. As the gas flow rates are generally kept constant, the flame temperature is reduced to being a function of the torch power input only. From Figure 5-17 it can be seen that fusing remains below 10 % up to about 9.5 kW (representing a flame temperature of approximately 1350 K), but increases dramatically to 30 % when power is raised above 9.5 kW to 10.5 kW (representing a flame temperature of 1450 K).

Just as the flame temperature affects the degree of fusing, the run duration was also expected to have a substantial effect. As the run duration is increased more particles pass through the flame more often, allowing for more opportunity to sinter and fuse. This is shown in Figure 5-18 where the degree of fusing increases directly with increasing run duration. Up to 10 minutes at a power input of 9.0 kW (flame temperature of 1300 K), fusing is limited to 2 %. An increase in run duration to 40 minutes raises the degree of fusing to 18 % at the same flame temperature. This is due to the following: the flame temperature is not fully uniform, there are areas where the air has not mixed as well as in others, resulting in higher temperatures. Thus, some particles pass through these hotter areas and fuse. As time increases, more particles pass through these areas, resulting in increased fusing. In addition to improving the circulation of

the particles, improving the degree of air/plasma flame mixing is also recommended.

CHAPTER VII

CONCLUSIONS & RECOMMENDATIONS

1. Conclusions

The primary conclusion of this work is that the desired calcination reaction of the vanadium ore concentrate can be realized in the designed equipment. Substantial conversions were obtained while at the same time the operation of the equipment remained simple enough to be handled by one person.

It was found that with the constructed system, the smaller particle size (d_p = 40 microns) could not be spouted on a consistent basis. The larger particles (d_p = 70 microns) could be 'bubble-spouted', which provided acceptable circulation over a range of parameters. With bed temperatures increasing over 700°C, it was found that circulation was not sufficient and excessive fusing of the particles resulted.

It was found that the bed temperature had a substantial effect on the degree of conversion of vanadium pentoxide to sodium metavanadate. With a final bed temperature increase from 500°C to almost 700°C, the degree of conversion improved from 10% to 33%. At the same time, the effect of run duration was less pronounced. Though the smaller particles provided unsatisfactory operation, it was shown that smaller particles result in higher conversions.

It was shown that the use of larger particles resulted in lower salt losses than with the smaller particles. Salt losses reached 34% and 54% respectively. From salt mass distributions in the bed it was shown that salt losses are mostly due to evaporation.

Particle entrainment was found to level off at approximately 8% with the larger particles. With the smaller particles, entrainment reached as high as 30%. Since entrainment leveled off with time it seems that attrition of particles is not significant.

2. Recommendations

The major problem encountered was fusing of particles due to poor circulation. Fusing became excessive at temperatures above 700°C, halting circulation of the particles. With the smaller particles, fusing presented a problem at all conditions. A means of improving the circulation of the particles must be implemented.

What is presently in the design stage for the second part of this project is a spout-fluid bed. Such a unit will incorporate a central hot spout from the torch with a surrounding fluidized area effected by the necessary air. With this arrangement, all particles will flow much more readily and will thus circulate better. A suggested schematic of this spout-fluid bed is given in Figure 7-1.

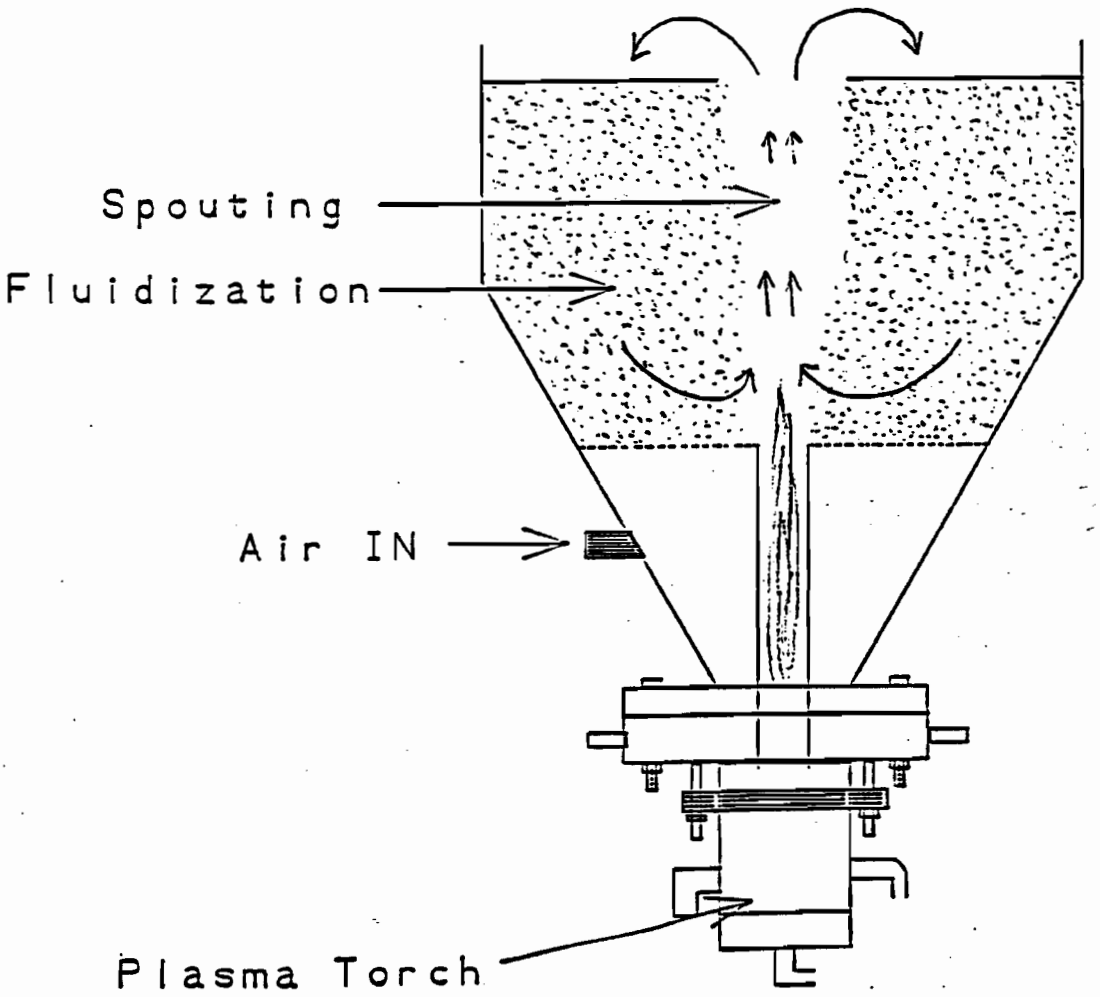

Figure 7-1 - Proposed Spout-Fluid Bed Design

REFERENCES

References

1. Alcock, C.B., "Plasma Processing of Oxide Systems in the Temperature Range 1000-3000K", Pure & Applied Chemistry, vol. 52. Pergamon Press Ltd., London, 1980, pp. 1817-1827.

2. Baddour, Raymond F., Robert S. Timmins, "The Application of Plasmas to Chemical Processing". The M.I.T. Press. Cambridge, 1967.

3. Bokhari, A., M. Boulos, "Energy Balance for a DC Plasma Torch", Can. Jour. of Chem. Eng., vol. 58, April 1980, pp. 171-176.

4. Bonet, C., et al, "A Study of the Thermal Treatment of Refractories in a Fluidized Bed by Plasma Discharge", Rev. Int. Htes. Temp. Refract., vol. 11, pp. 11-24, 1974.

5. Bonet C., "Thermal Plasma Processing", Chemical Engineering Progress, December 1976, pp. 63-69.

6. Boulos, M.I., W.H. Gauvin, "Powder Processing in a Plasma Jet: A Proposed Model", Pure & Applied Chemistry, vol. 52, Pergamon Press Ltd., London, 1980.

7. Burwell, B., "Extractive mettalurgy of vanadium", Journal of Metals, August 1961, pp. 562-570.

8. Chang, C.W., J. Szekely, "Plasma Applications in Metals Processing", Journal of Metals, February 1980, pp. 57-64.

9. Cole, Sandford S., & John S. Breitenstein, "Recovery of Vanadium from Titaniferous Magnetite", Journal of Metals, December 1951, pp. 1133-1137.

10. Ettlinger, Lester A., T. Daniel Nainan, Robert P. Ouelette, Paul A. Cheremisinoff, "High-Temperature Plasma Technology Applications" Electrotechnology, Volume 6. Ann Arbor Science. Ann Arbor, Michigan, 1980.

11. Fauchais, P., E. Bourdin, J.F. Coudert, "Generalities on the Physical and Chemical Processes in a Thermal Plasma", Int. Chem. Eng., 23(2), April 1983, pp. 238-264.

12. Gabra, G., & I. Malinsky, "A comparative study of the extraction of vanadium from titaniferous magnetite and slag", Proceedings of the 110th AIME meeting, Chicago, Illinois, February 22-26, 1981.

13. Gerdeman, D.A., N.L. Hecht, "Arc Plasma Technology In Materials Science". Springer Verlag. New York, 1972.

14. Goddard, John B., & Joseph S. Fox, "Salt roasting of vanadium ores", Proceedings of the 110th AIME meeting, Chicago, Illinois, February 22-26, 1981.

15. Hamblyn, S.M.L., "Plasma Technology and its Application to Extractive Metallurgy", Minerals Science Engineering, 9, No. 3, July 1977, pp. 151-176.

16. Hollahan, John R., T. Bell Alexis, "Techniques and Applications of Plasma Chemistry", John Wiley and Sons, New York, 1974.

17. Ibberson, V.J., M.W. Thring, "Plasma Chemical and Process Engineering", Ind. and Eng. Chem., November 1969, pp. 48-61.

18. Instrumentation Laboratory Inc., Analytical Instrument Division, "Operator's Manual, Model IL 357 & 457 AA/AE Spectrophotometer", Dec. 1975.

19. Jones, M.J. editor, "Advances in Extractive Metallurgy and Refining", The Institution of Mining and Metallurgy, London, 1972.

20. Jurewicz, Jerzy, Pierre Proulx, Maher I. Boulos, "The Plasma Spouted Bed Reactor". Paper presented at ISPC-7, Eindhoven, July 1-5, 1985.

21. Kubanek, G.R., W.H. Gauvin, G.A. Irons, H.K. Choi, "The Industrial Application of Plasmas to Metallurgical Processes", 4th International Symposium on Plasma Chemistry, Zurich, Switzerland, August 1979.

22. Liang, Anita D., "Ferroniobium Production by Plasma Technology - A Techno Economic Assessment", M.Eng. Thesis, McGill University, 1982.

23. MacRae, Donald R., Richard G. Gold, C. Douglas Thompson, William R. Sandall, "Ferrovanadium Production by Plasma Carbothermic Reduction of Vanadium Oxide" 34th Electric Furnace Conference, St. Louis, Missouri, December 1976.

24. Malinsky, Ivan, Gerard Castonguay, "Dossier Vanadium", Centre des Recherches Minérales, Québec, October 5, 1983.

25. Malinsky, I., & R. LeHouillier, "Traitement d'un gisement de

magnétite titanifère et vanadifère", Canad. Met. Quarterly (Annual volume of CIM), 17, 1978, pp. 108-113.

26. Maske, K.U., J.J. Moore, "The Application of Plasmas to High Temperature Reduction Metallurgy", High Temperature Technology, August 1982, pp. 51-63.

27. Masterloy Products Limited, "Beneficiation of vanadium-containing slags", Canadian Patent, June 1, 1971.

28. Munz, Richard J., Personal Consultations.

29. Munz, R.J., "Plasma Spouted Bed Calcination of Lac Doré Vanadium Concentrate", research proposal submitted to the Centre de Recherches Minerales, Montreal, 27. Nov. 1984.

30. Patterson, Peter A., "Laser Doppler Anemometry in a Transferred-Arc Plasma", Master's Thesis, McGill University, submitted August 1983.

31. Rykhalin, N.N., "Thermal Plasmas in Extractive Metallurgy", Pure & Applied Chemistry, vol. 52. Pergamon Press Ltd., London, 1980, pp. 1801-1815.

32. Saha, A.K., R.N. Misra, P.P. Bhatnagar, "Studies on Extraction of Vanadium by Fluo-solid Salt Roasting", NML Technical Journal, February 1969, pp. 6-11.

33. Spink, D.R., G.L. Rempel, & C.O. Gomez-Bueno, "Extraction of Vanadium from Athabasca Tar Sands Fly Ash", Proceedings of the 110th AIME Meeting, February 22-26, 1981.

34. Stuart, Paul R., "Synthesis Gas Production from Peat using a Steam Plasma", Master's Thesis, McGill University, submitted January 1984.

35. Szente, Roberto N., "Cathode Erosion in Magnetically Rotated Arcs", Master's Thesis, McGill University, submitted May 1986.

36. Waldie, B., "Review of Recent Work on the Processing of Powders in High Temperature Plasmas Part I - Processing and Economic Studies", The Chemical Engineer, March 1972, pp. 92-96.

37. Waldie, B., "Review of Recent Work on the Processing of Powders in High Temperature Plasmas Part II - Particle Dynamics, Heat Transfer and Mass Transfer", The Chemical Engineer, May 1972, pp. 188-193.

38. Zanetti, Richard J., "Plasma: Warming up to new CPI Applications", Chemical Engineering, December 26, 1983, pp. 14-17.

39. Handbook of Chemistry and Physics, 66th Edition. CRC Press 1985.

40. Mathur, Kishan & Norman Epstein, "Spouted Beds", New York: Academic Press, 1974.

APPENDICES

A. Procedure Checklist

____1. Check whether the right set of power lines are connected. (i.e. <u>not</u> Paul Stuart's* lines)

____2. Check the proper polarity of the cables.

____3. Check isolation of + and - (approx. 1500 Ω)

____4. Check whether the power cables are not in contact anywhere between the control console and the torch.

____5. Check whether the apparatus is properly grounded.

____6. Check whether all water cooling lines are connected.

____7. Start the water cooling for all components and verify that a proper water flow reaches all of them.

____8. Check for any water leaks.

____9. Check that all three of Paul S's** gas valves are closed

____10. Start the gas flow and verify that it reaches the torch. (i.e. <u>not</u> Paul Stuart's torch)

____11. Start the air flow and verify that it reaches the reactor.

____12. Check for leaks in the gas and air lines

____13. Turn off the gas flow.

*Power console is shared with Paul Stuart
**Air lines are coupled with Paul Stuart's equipment

B. F*A*C*T Print-outs

```
V205 + 3.75NA*CL =
(1100,1) (1100,1)
~

                0.500  (      .999        V*O*CL3
                       +      .633E-03    NA*CL
                       +      .290E-03    NA2CL2
                       +      .239E-03    V*CL4
                       +      .696E-04    CL2
                       +      .124E-04    CL
                       +      .969E-10    O2
                       +      .621E-11    CL*O
                       +      .111E-12    NA
                       +      .243E-13    O
                       +      .513E-16    CL2O
                       +      .138E-17    V*O
                       +      .576E-18    NA*O
                       +      .675E-20    O2CL
                       +      .404E-25    O3
                       +      .454E-26    NA2
                       +      .510E-29    V                    )
                                          (1100.0, 1.00    ,G )

                       +      .750        (NA2O)*(V2O5)
                                          (1100.0, 1.00    ,S1)

                       +     2.25         NA*CL
                                          (1100.0, 1.00    ,S1)
```

V_2O_5 reacting with NaCl

```
0.756  {      .992          O2
          +   .754E-02      C*O2
          +   .247E-07      O
          +   .186E-07      NA
          +   .788E-08      NA*O
          +   .155E-09      O3
          +   .132E-09      C*O
          +   .614E-16      NA2
          +   .403E-42      C
          +   .996E-51      C3O2
          +   .140E-64      C2
          +   .0            C3
          +   .0            C4
          +   .0            C5                    }
                            (1200.0, 1.00    ,G )

          +   .994          NA2C*O3
                            (1200.0, 1.00    ,L1)

          +   .570E-02      (NA2O)*(FE2O3)
                            (1200.0, 1.00    ,S1)

          +   .0            FE3O4
                            (1200.0, 1.00    ,S2)

          +   1.49          FE2O3
                            (1200.0, 1.00    ,S3)

          +   .0            FE3C
                            (1200.0, 1.00    ,S2)

          +   .0            FE
                            (1200.0, 1.00    ,S2)

          +   .0            NA2O
                            (1200.0, 1.00    ,S2)
```

Ilmenite reacting with Na_2CO_3

```
0.000  {      .857        C*O
          +   .143        C*O2
          +   .509E-05    NA
          +   .960E-11    NA2
          +   .130E-12    C3O2
          +   .595E-15    NA*O
          +   .546E-18    O
          +   .489E-19    O2
          +   .287E-24    TI*O
          +   .601E-26    G
          +   .263E-28    C3
          +   .772E-30    C2
          +   .167E-33    TI
          +   .269E-36    C4
          +   .143E-36    C5
          +   .457E-39    O3                    }
                          (1100.0, 1.00    ,G )

          +   .0          NA
                          (1100.0, 1.00    ,L1)

          +   1.00        (FE*O)*(TI*O2)
                          (1100.0, 1.00    ,S1)

          +   .0          FE2TI
                          (1100.0, 1.00    ,S1)

          +   .0          FE*TI
                          (1100.0, 1.00    ,S1)

          +   .162E-05    (NA2O)*(FE2O3)
                          (1100.0, 1.00    ,S1)

          +   .0          (NA2O)*(TI*O2)3
                          (1100.0, 1.00    ,S1)

          +   .0          (NA2O)*(TI*O2)2
                          (1100.0, 1.00    ,S1)

          +   .458E-05    (NA2O)*(TI*O2)
                          (1100.0, 1.00    ,S2)

          +   .0          TI*O2
                          (1100.0, 1.00    ,S1)

          +   1.00        NA2C*O3
                          (1100.0, 1.00    ,S2)

          +   .0          NA2O
                          (1100.0, 1.00    ,S2)
```

Magnetite reacting with Na_2CO_3